Mechanics Research Communications 156 (2026) 104770

Contents lists available at ScienceDirect

Mechanics Research Communications

journal homepage: www.elsevier.com/locate/mechrescom

Scaling as a selection principle for asymptotic chemoelastic interface laws☆,☆☆

Raffaella Rizzoni

Department of Engineering, University of Ferrara, Via Saragat 1, Ferrara, 44122, Italy

ARTICLE INFO

Keywords:
Asymptotic analysis
Thin interphase
Imperfect interface
Chemoelasticity
Chemo-mechanical coupling
Surface excess

ABSTRACT

Asymptotic interface laws are calculated to replace vanishingly linear chemo-mechanical interphases. The elastic, chemical, transport, and chemo-mechanical coupling parameters of the interphase are scaled with the thickness parameter. Different scalings lead to distinct transmission regimes. The limit models include perfect, resistive, imperfect, and coupled chemo-mechanical interfaces. The main original feature is the identification of a coupled regime in which mechanical imperfectness, chemical storage, and species exchange remain linked at the limit interface. In this regime, the displacement and flux jumps are coupled, allowing the interface to exchange chemical species with the adherents. This behavior is interpreted as an interfacial excess contribution that emerges from the asymptotic reduction of the thin interphase. A one-dimensional example shows that, unlike the other regimes, the coupled interface law activates a transient chemical perturbation near the interface and induces a rate-dependent response to loading. The study emphasizes the role of scaling as a selection principle for chemoelastic interface laws and highlights its relevance for the reduced modeling of thin multiphysical interphases.

1. Introduction

Thin interphases occur in a wide range of natural and engineered heterogeneous systems and play a key role in their mechanical and transport responses. In engineering applications, for instance, thin interphases arise in adhesive joints, coatings, layered composites, and functional materials. Adhesive connections in composite structures provide a typical example in which the geometry and behavior of the adhesive layer influence the structural response [1,2]. In biomedical and biomechanical contexts, interfacial regions are also relevant at tissue–implant interfaces, where the implant surface roughness and the partial contact between bone tissue and the implant play a central role in the mechanical response [3].

When their thickness is small compared to the characteristic dimensions of the structure, the numerical model of thin interphases can be computationally expensive. A classic approach to accounting for their influence is to replace them with equivalent interfaces across which suitable transmission conditions on the jumps of the displacement and traction fields are prescribed. These reduced models are calculated to have the same leading-order behavior of the interphase, and they eliminate the small geometric scale from the problem.

The asymptotic derivation of interface laws has been extensively developed in solid mechanics and has become a standard tool for obtaining reduced models of thin interphases. Classical contributions include the imperfect interface models of Hashin [4,5] and the equivalent interface descriptions of Benveniste and Miloh [6], while asymptotic derivations for thin adhesive layers and bonded joints were developed, among others, by Klarbring [7] and by Geymonat, Krasucki and Lenci [8].

More recently, thin elastic adhesive layers have been shown to lead to perfect, soft, hard, and higher-order interface laws. These laws depend on the relative stiffness of the interphase with respect to the adherents [9–11]. Frédéric Lebon has made influential contributions to this line of research, which has played an important role in clarifying how interface laws can be obtained from asymptotic thin-layer models instead of being phenomenologically prescribed. This asymptotic viewpoint has also been extended to other classes of imperfect interfaces, including viscoelastic interfaces [12], stochastic interface models [13], rough contact surfaces [14], and coupled frameworks, including poroelastic, linear multiphysics and thermoelastic composites [15–18]. Related atypical conditions were recently derived for thin poroelastic

☆ This article is part of a Special issue entitled: 'Multi. Asympt. Meth. Solid Mech.' published in Mechanics Research Communications.
☆☆ To Frédéric Lebon, on the occasion of his 65th birthday.
E-mail address: raffaella.rizzoni@unife.it.

https://doi.org/10.1016/j.mechrescom.2026.104770
Received 30 May 2026; Received in revised form 3 July 2026; Accepted 15 July 2026
Available online 21 July 2026
0093-6413/© 2026 The Author. Published by Elsevier Ltd. This is an open access article under the CC BY license (http://creativecommons.org/licenses/by/4.0/).

interphases, where non-proportional scalings lead to coupled transmission laws [18]. These studies show that limit interface laws result from specific scalings of the material properties with the layer thickness.

In the chemo-mechanical setting, mechanical deformation may be coupled with transport phenomena, such as diffusion driven by chemical potential gradients, as described in chemoelastic and diffusion–deformation theories [19–21]. Such couplings arise in several classes of materials and degradation processes, including gels, polymeric adhesives, coatings, battery materials, and environmentally assisted cracking phenomena such as stress corrosion cracking [22–25].

In this context, the interphase may not only transmit mechanical tractions and chemical fluxes, but may also store, release, or exchange chemical species with the surrounding bulk phases. This interpretation is related to the classical notion of surface excess in physical chemistry [26]. Coupled chemo-mechanical interface models have recently received increasing attention. Zhou et al. proposed a finite-deformation chemo-mechanical cohesive model for imperfect interfaces in heterogeneous composites, accounting for displacement jumps, chemical potential jumps and mass flux jumps across the interface [27]. Auth et al. developed a chemo-mechanical cohesive zone formulation for environmentally assisted interfacial degradation, with particular attention to the coupling between diffusion, cohesive strength degradation and fracture [28]. More recently, D'Andréa et al. introduced a fully coupled thermo-chemo-mechanical traction–separation interface model including chemical bonding, damage, friction and possible interface formation [29].

These contributions show the relevance of coupled interface descriptions in chemo-mechanical and thermo-chemo-mechanical problems. However, they are based on cohesive or traction–separation interface formulations in which the zero-thickness interface law is introduced directly. In contrast, the purpose of the present work is to derive effective transmission conditions from a thin linear chemoelastic interphase by asymptotic analysis. In this framework, the elastic, chemical, mobility and coupling parameters of the interphase may scale independently with the thickness, and different scalings may select distinct limit interface laws.

To explore these issues, the thin interphase is placed between two chemoelastic adherents and its thickness is assumed to vanish with a small parameter ε. The elastic tensor, the chemo-mechanical coupling tensor, the chemical modulus, and the mobility tensor of the interphase are allowed to scale with ε. The role of scaling is central in the present analysis. The dependence of the interphase parameters on ε is introduced as an asymptotic tool to explore the effects arising from different balances between elasticity, mass transport, and chemo-mechanical coupling. The resulting interface laws should therefore be interpreted as limiting models associated with different physical regimes, rather than as the consequence of an actual dependence of material properties on thickness. In this sense, scaling acts as a selection principle, determining which physical mechanisms survive and which vanish in the limit.

Four representative regimes are considered in this study. When the material parameters of the interphase are independent of the small parameter, the thin layer behaves, at leading order, as a perfect interface (regime I). When the mobility is linearly scaled with the thickness while the other material parameters are independent of ε, a chemically resistive interface is obtained, whereas the mechanical transmission remains perfect (regime II). When all the constitutive parameters linearly scale with the thickness, the limit transmission conditions correspond to uncoupled imperfect mechanical and chemically resistive interface laws (regime III). This regime is the chemoelastic counterpart of the order-zero soft thermoelastic case derived in [17]. Finally, when the elastic, chemical, and coupling parameters scale with the thickness while the mobility remains independent of ε, coupled chemo-mechanical imperfect interface laws are obtained (regime IV).

This fourth regime is one of the original contributions of the present study. In this case, the limit law produces a coupled interface condition in which the mechanical jump, the chemical state at the interface, and the jump of normal flux are linked. As a consequence, the interface can exchange species with the adherents and the resulting chemo-mechanical response is rate-dependent. This behavior is similar to the classical notion of surface excess in physical chemistry [26]. In the present setting, however, the excess is not introduced as an additional bulk concentration field or through a separate surface free energy. It appears through the interfacial species balance: the jump of the normal flux is balanced by the time derivative of an interfacial amount per unit area. This interfacial amount depends on the interfacial chemical potential and, through the chemo-mechanical coupling, on the jump of the displacement field. In this sense, the limit interface acts as a reduced phase that carries its own excess amount and exchanges species with the adjacent bulk phases. Notably, this contribution is not phenomenologically postulated, but is obtained as the limit of a thin chemoelastic interphase for the specific scaling of the material parameters.

The effect of the different interface laws is illustrated through a one-dimensional example. A composite bar made of two identical chemoelastic adherents joined by one of the limit interfaces is subjected to a time-dependent tensile load under chemically sealed external boundary conditions. The example shows that, under the considered loading, the first three regimes lead to a spatially uniform chemical response in the adherents, whereas the fourth regime introduces a transient chemical perturbation localized near the interface. This perturbation is associated with species exchange between the limit interface and the adherents and affects the mechanical response, making the macroscopic stress–strain response rate-dependent.

The paper is organized as follows. Section 2 introduces the chemoelastic formulation in the adherents and in the thin interphase. Section 3 presents the asymptotic analysis associated with the four different scalings of the interphase parameters. The resulting transmission conditions are summarized in Section 4. Section 5 illustrates the different behavior of the composite bar under the four interfacial regimes. Final remarks and possible extensions are given in the conclusion.

2. Notation and governing equations

Let $(O,\mathbf{i}_1,\mathbf{i}_2,\mathbf{i}_3)$ be an orthonormal Cartesian frame, and let $\mathbf{x} := (x_1,x_2,x_3)$ denote the coordinates of a material point. Given a bounded regular set $S \subset \mathbb{R}^2$, consider a composite body occupying the domain Ω^ε, consisting of a thin interphase Ω_i^ε of small thickness $h^\varepsilon = \varepsilon h$, $0 < \varepsilon \ll 1$, with

$$\Omega_i^\varepsilon = \left\{ (x_1,x_2,x_3) \in \mathbb{R}^3 : (x_1,x_2) \in S,\ |x_3| < \frac{\varepsilon h}{2} \right\},$$

sandwiched between two adherents, with heights H^+ and H^-, defined as

$$\Omega_\pm^\varepsilon = \left\{ (x_1,x_2,x_3) \in \mathbb{R}^3 : (x_1,x_2) \in S, H^\pm + \frac{\varepsilon h}{2} \geq \pm x_3 > \frac{\varepsilon h}{2} \right\}.$$

The total domain is given by $\Omega^\varepsilon = \Omega_-^\varepsilon \cup \Omega_i^\varepsilon \cup \Omega_+^\varepsilon$. The adherents are perfectly bonded to the thin interphase along the common interfaces

$$S_\pm^\varepsilon = \left\{ (x_1,x_2,x_3) \in \mathbb{R}^3 : (x_1,x_2) \in S,\ x_3 = \pm\frac{\varepsilon h}{2} \right\}.$$

In the following, a subscript k, with $k \in \{-,i,+\}$, will be taken to denote the restriction of a field to the subdomain Ω_k^ε.

The three domains Ω_k^ε are composed of linear chemoelastic materials considered in the classical sense of diffusion-induced elastic response [19,30]. For simplicity, a single diffusing chemical species is assumed. The governing variables for the chemo-mechanical problem are the displacement field, $\mathbf{u}_k^\varepsilon(\mathbf{x},t)$, and the chemical potential field, $\mu_k^\varepsilon(\mathbf{x},t)$, with $\mathbf{x}$ denoting a material point in Ω_k^ε and t an instant in a time interval $[0,T)$.

Initially, the composite body is assumed in a natural reference state, characterized by being undeformed, stress-free, and at a uniform chemical potential μ_0. This corresponds to the initial conditions:

$$\mathbf{u}_k^\varepsilon(\mathbf{x},0) = \mathbf{0},$$

$$\boldsymbol{\sigma}_k^\epsilon(\mathbf{x},0)=\mathbf{0},$$
$$\mu_k^\epsilon(\mathbf{x},0)=\mu_0, \tag{1}$$

where $\boldsymbol{\sigma}_k^\epsilon$ is the symmetric Cauchy stress tensor in Ω_k^ϵ. Let $\mathbf{e}(\mathbf{u}^\epsilon)=\frac{1}{2}\left(\nabla\mathbf{u}^\epsilon+(\nabla\mathbf{u}^\epsilon)^T\right)$ be the linearized strain tensor. In each subdomain Ω_k^ϵ, let c_k^ϵ and $\mathbf{j}_k^\epsilon$ denote, respectively, the concentration and the rate of flow of the diffusing species. The constitutive equations are given by

$$\begin{aligned}\boldsymbol{\sigma}_k^\epsilon&=\mathbb{C}_k^\epsilon\mathbf{e}(\mathbf{u}_k^\epsilon)+\tilde{c}_k^\epsilon\,\mathbf{S}_k^\epsilon,\\ \tilde{\mu}_k^\epsilon&=\mathbf{S}_k^\epsilon\cdot\mathbf{e}(\mathbf{u}_k^\epsilon)+\Lambda_k^\epsilon\tilde{c}_k^\epsilon,\\ \mathbf{j}_k^\epsilon&=-\mathbf{M}_k^\epsilon\nabla\mu_k^\epsilon,\end{aligned} \tag{2}$$

with $\tilde{\mu}_k^\epsilon:=\mu_k^\epsilon-\mu_0$ and $\tilde{c}_k^\epsilon:=c_k^\epsilon-c_{k0}^\epsilon$, where c_{k0}^ϵ is the reference species concentration in the subdomain Ω_k^ϵ. The terms $\mathbb{C}_k^\epsilon$, $\mathbf{S}_k^\epsilon$, Λ_k^ϵ and $\mathbf{M}_k^\epsilon$ are, respectively, the fourth-order elasticity tensors, the second order chemo-mechanical coupling tensors, the chemical moduli and the second order mobility tensors at the reference concentrations c_{k0}^ϵ. The following properties are assumed: the elasticity tensors $\mathbb{C}_k^\epsilon$ have minor and major symmetries and are positive definite, the chemo-mechanical coupling tensors $\mathbf{S}_k^\epsilon$ are symmetric, the mobility tensors $\mathbf{M}_k^\epsilon$ are symmetric and positive definite, and the chemical moduli Λ_k^ϵ are positive. Moreover, the drained elasticity tensors [19]

$$\mathbb{C}_k^{\epsilon,dr}:=\mathbb{C}_k^\epsilon-\frac{1}{\Lambda_k^\epsilon}(\mathbf{S}_k^\epsilon\otimes\mathbf{S}_k^\epsilon), \tag{3}$$

are assumed to be positive definite. These assumptions are compatible with the standard thermodynamic framework for coupled diffusion–mechanics processes [30].

The analysis is restricted to quasi-static processes where the effects of inertia are negligible compared to diffusion. Body forces are neglected in the interphase, while they are denoted by $\mathbf{b}_k^\epsilon(\mathbf{x},t)$ in the adherents. The governing equations in the composite domain Ω^ϵ consist of the local species mass balance

$$\dot{\tilde{c}}_k^\epsilon+\mathrm{Div}\,\mathbf{j}_k^\epsilon=0,\quad \text{in } \Omega_k^\epsilon,\qquad k\in\{-,i,+\}. \tag{4}$$

and the local balance of linear momentum, with inertia neglected,

$$\begin{aligned}&\mathrm{Div}\,\boldsymbol{\sigma}_k^\epsilon+\mathbf{b}_k^\epsilon=\mathbf{0},\quad \text{in } \Omega_k^\epsilon,\qquad k\in\{-,+\},\\ &\mathrm{Div}\,\boldsymbol{\sigma}_i^\epsilon=\mathbf{0},\quad \text{in } \Omega_i^\epsilon,\end{aligned} \tag{5}$$

supplemented by suitable boundary and interface conditions specified below.

For the mechanical boundary conditions, the external boundary of the adherents $\partial\Omega_{ext}^\epsilon:=\partial\Omega_+^\epsilon\cup\partial\Omega_-^\epsilon\setminus\{S_+^\epsilon\cup S_-^\epsilon\}$ is decomposed as

$$\partial\Omega_{ext}^\epsilon=\Gamma_u^\epsilon\cup\Gamma_s^\epsilon,\qquad \Gamma_u^\epsilon\cap\Gamma_s^\epsilon=\emptyset.$$

Dirichlet boundary conditions are prescribed on Γ_u^ϵ, while Neumann boundary conditions are imposed on Γ_s^ϵ:

$$\begin{aligned}\mathbf{u}^\epsilon&=\mathbf{0}\quad \text{on } \Gamma_u^\epsilon,\\ \boldsymbol{\sigma}^\epsilon\mathbf{n}&=\mathbf{s}^\epsilon\quad \text{on } \Gamma_s^\epsilon,\end{aligned} \tag{6}$$

with $\mathbf{s}^\epsilon(\mathbf{x},t)$ a prescribed surface force. For the chemical boundary conditions, $\partial\Omega_{ext}^\epsilon$ is decomposed as

$$\partial\Omega_{ext}^\epsilon=\Gamma_{\tilde{\mu}}^\epsilon\cup\Gamma_j^\epsilon,\qquad \Gamma_{\tilde{\mu}}^\epsilon\cap\Gamma_j^\epsilon=\emptyset,$$

and the following conditions are prescribed:

$$\begin{aligned}\tilde{\mu}^\epsilon&=0\quad \text{on } \Gamma_{\tilde{\mu}}^\epsilon,\\ \mathbf{j}^\epsilon\cdot\mathbf{n}&=\check{j}^\epsilon\quad \text{on } \Gamma_j^\epsilon,\end{aligned} \tag{7}$$

with $\check{j}^\epsilon(\mathbf{x},t)$ the prescribed outward flux. On the lateral boundary of the adhesive interphase, $\Gamma_{lat}^\epsilon:=\partial\Omega_i^\epsilon\setminus\{S_+^\epsilon\cup S_-^\epsilon\}$, the following mechanical and chemical conditions are prescribed:

$$\begin{aligned}\boldsymbol{\sigma}^\epsilon\mathbf{n}&=0,\\ \mathbf{j}^\epsilon\cdot\mathbf{n}&=0.\end{aligned} \tag{8}$$

At the interfaces $S_\pm^\epsilon$, perfect mechanical and chemical bonding is assumed

$$\begin{aligned}&[\![\mathbf{u}^\epsilon]\!]=\mathbf{0},\quad [\![\boldsymbol{\sigma}^\epsilon\mathbf{i}_3]\!]=\mathbf{0},\\ &[\![\tilde{\mu}^\epsilon]\!]=0,\quad [\![\mathbf{j}^\epsilon\cdot\mathbf{i}_3]\!]=\mathbf{0},\end{aligned} \tag{9}$$

where $[\![\cdot]\!]$ denotes the jump across the interface S_+^ϵ or S_-^ϵ.

The admissible spaces for the displacement and chemical potential fields are defined as

$$\begin{aligned}\mathcal{V}_u^\epsilon&=\{\mathbf{u}\in[H^1(\Omega^\epsilon)]^3\mid\mathbf{u}=\mathbf{0}\text{ on }\Gamma_u^\epsilon\},\\ \mathcal{V}_{\tilde{\mu}}^\epsilon&=\{\tilde{\mu}\in H^1(\Omega^\epsilon)\mid\tilde{\mu}=0\text{ on }\Gamma_{\tilde{\mu}}^\epsilon\}.\end{aligned} \tag{10}$$

The associated spaces of admissible variations are $\mathcal{V}_{u,0}^\epsilon=\mathcal{V}_u^\epsilon$ and $\mathcal{V}_{\tilde{\mu},0}^\epsilon=\mathcal{V}_{\tilde{\mu}}^\epsilon$. For compactness, the vector of unknowns $\mathbf{w}_k^\epsilon=(\mathbf{u}_k^\epsilon,\tilde{\mu}_k^\epsilon)$ is introduced, belonging to $\mathcal{V}_u^\epsilon\times\mathcal{V}_{\tilde{\mu}}^\epsilon$, and the corresponding vector of test functions $\boldsymbol{\eta}=(\mathbf{v},\xi)$ is introduced, belonging to $\mathcal{V}_{u,0}^\epsilon\times\mathcal{V}_{\tilde{\mu},0}^\epsilon$.

Starting from the balance equations, and applying a standard procedure, the weak formulation of the chemoelastic problem can be obtained: find $\mathbf{w}^\epsilon$ such that for all admissible $\boldsymbol{\eta}^\epsilon$ and for all $t\in[0,T)$,

$$a^\epsilon(\mathbf{w}^\epsilon,\boldsymbol{\eta})+b^\epsilon(\dot{\mathbf{w}}^\epsilon,\boldsymbol{\eta})=l^\epsilon(\boldsymbol{\eta}) \tag{11}$$

where a^ϵ is the bilinear form

$$\begin{aligned}a^\epsilon(\mathbf{w}^\epsilon,\boldsymbol{\eta}):=\sum_{k\in\{-,i,+\}}\Bigg\{&\int_{\Omega_k^\epsilon}\left(\mathbb{C}_k^{\epsilon,dr}\mathbf{e}(\mathbf{u}_k^\epsilon)+\frac{1}{\Lambda_k^\epsilon}\tilde{\mu}_k^\epsilon\mathbf{S}_k^\epsilon\right)\cdot\mathbf{e}(\mathbf{v}_k^\epsilon)\,dV\\ &+\int_{\Omega_k^\epsilon}\mathbf{M}_k^\epsilon\nabla\tilde{\mu}_k^\epsilon\cdot\nabla\xi_k\,dV\Bigg\}.\end{aligned} \tag{12}$$

and b^ϵ is the following bilinear form

$$b^\epsilon(\dot{\mathbf{w}}^\epsilon,\boldsymbol{\eta}):=\sum_{k\in\{-,i,+\}}\int_{\Omega_k^\epsilon}\frac{1}{\Lambda_k^\epsilon}\left(\dot{\tilde{\mu}}_k^\epsilon-\mathbf{S}_k^\epsilon\cdot\dot{\mathbf{e}}(\mathbf{u}_k^\epsilon)\right)\xi_k\,dV. \tag{13}$$

In (11), the linear form l^ϵ collects the external mechanical and chemical loadings

$$l^\epsilon(\boldsymbol{\eta})=\sum_{k\in\{-,+\}}\int_{\Omega_k^\epsilon}\mathbf{b}_k^\epsilon\cdot\mathbf{v}_k^\epsilon dV+\int_{\Gamma_s^\epsilon}\mathbf{s}^\epsilon\cdot\mathbf{v}^\epsilon dS-\int_{\Gamma_j^\epsilon}\check{j}^\epsilon\xi\,dS. \tag{14}$$

Under the above assumptions, the bilinear forms a^ϵ and b^ϵ are continuous on the corresponding admissible spaces, and the linear form l^ϵ is continuous on $\mathcal{V}_{u,0}^\epsilon\times\mathcal{V}_{\tilde{\mu},0}^\epsilon$. Moreover, provided that Γ_u^ϵ and $\Gamma_{\tilde{\mu}}^\epsilon$ have positive measure, the elastic and diffusion contributions define coercive bilinear forms on the corresponding displacement and chemical-potential spaces. The resulting weak problem has the standard structure of a coupled quasi-static diffusion–mechanics system. Rigorous existence and uniqueness results for closely related coupled systems are available in the literature for fully coupled quasi-static thermo-poroelastic systems [31], and for diffusion–mechanics systems [32].

3. Asymptotic analysis

Due to the small thickness of the adhesive interphase, ϵh, the solution of the chemoelastic problem is sought at each time instant using asymptotic expansions with respect to the small parameter ϵ, $0<\epsilon\ll1$. The first step in the asymptotic analysis is to rescale the thin domain to introduce a domain of fixed thickness h. This can be achieved via the classical procedure described in [33] and introduced in the following subsection.

3.1. Rescaled formulation

The following changes of variables transform the problem from the physical configuration in coordinates (x_1,x_2,x_3) to a rescaled configuration in coordinates (z_1,z_2,z_3)

- in the interphase, the domain Ω_i^ε is mapped to the fixed domain $\Omega_i = \{(z_1, z_2, z_3) \in \mathbb{R}^3 : (z_1, z_2) \in S, |z_3| < \frac{h}{2}\}$. The mapping $\hat{\pi}^\varepsilon : \Omega_i^\varepsilon \to \Omega_i$ is a rescaling defined as

  $$(z_1, z_2, z_3) = \hat{\pi}^\varepsilon(x_1, x_2, x_3) := (x_1, x_2, \frac{x_3}{\varepsilon})$$

  Any field v defined on Ω_i^ε is transformed into a field $\hat{v}$ on Ω_i such that $\hat{v}(\mathbf{z}) = v(\mathbf{x})$.
- in the adherents, the domains $\Omega_\pm^\varepsilon$ are mapped to the fixed domains $\Omega_\pm = \{(z_1, z_2, z_3) \in \mathbb{R}^3 : (z_1, z_2) \in S, H^\pm + \frac{h}{2} > \pm z_3 > \frac{h}{2}\}$. The mappings $\bar{\pi}^\varepsilon : \Omega_\pm^\varepsilon \to \Omega_\pm$ are rigid translations defined as

  $$(z_1, z_2, z_3) = \bar{\pi}_\pm^\varepsilon(x_1, x_2, x_3) := (x_1, x_2, x_3 \pm h/2 \mp \varepsilon h/2)$$

  Any field $v_\pm$ on $\Omega_\pm^\varepsilon$ is transformed into a field $\bar{v}_\pm(\mathbf{z}) = v_\pm(\mathbf{x})$.

The applied body forces and prescribed boundary values are assumed to be defined on the fixed rescaled domains, independent of ε. They are denoted by $\bar{\mathbf{b}}_\pm$, $\bar{\mathbf{s}}$, and $\bar{\bar{j}}$.

Using the change of variables in the adhesive, we have

$$\frac{\partial(\cdot)}{\partial z_1} = \frac{\partial(\cdot)}{\partial x_1}, \qquad \frac{\partial(\cdot)}{\partial z_2} = \frac{\partial(\cdot)}{\partial x_2}, \qquad \frac{\partial(\cdot)}{\partial z_3} = \varepsilon\frac{\partial(\cdot)}{\partial x_3}, \tag{15}$$

for any function $(\cdot)$. The rescaled weak chemo-mechanical problem reads as follows:

$$\bar{a}_+^\varepsilon(\bar{\mathbf{w}}_+^\varepsilon, \boldsymbol{\eta}) + \bar{a}_-^\varepsilon(\bar{\mathbf{w}}_-^\varepsilon, \boldsymbol{\eta}) + \bar{b}_+^\varepsilon(\bar{\mathbf{w}}_+^\varepsilon, \boldsymbol{\eta}) + \bar{b}_-^\varepsilon(\bar{\mathbf{w}}_-^\varepsilon, \boldsymbol{\eta}) + \varepsilon\hat{a}^\varepsilon(\hat{\mathbf{w}}^\varepsilon, \boldsymbol{\eta}) + \varepsilon\hat{b}^\varepsilon(\hat{\mathbf{w}}^\varepsilon, \boldsymbol{\eta}) = \bar{l}(\boldsymbol{\eta}) \tag{16}$$

where

$$\bar{a}_\pm^\varepsilon(\bar{\mathbf{w}}_\pm^\varepsilon, \bar{\boldsymbol{\eta}}) = \int_{\Omega_\pm} \{\left(\mathbb{C}_\pm^{\varepsilon,dr}\mathbf{e}(\bar{\mathbf{u}}_\pm^\varepsilon) + \frac{1}{\Lambda_\pm^\varepsilon}\bar{\tilde{\mu}}_\pm^\varepsilon\mathbf{S}_\pm^\varepsilon\right) \cdot \mathbf{e}(\bar{\mathbf{v}}_\pm) + \mathbf{M}_\pm^\varepsilon\nabla\bar{\tilde{\mu}}_\pm^\varepsilon \cdot \nabla\bar{\tilde{\xi}}_\pm\} dV_z, \tag{17}$$

$$\bar{b}_\pm^\varepsilon(\bar{\tilde{\mathbf{w}}}_\pm^\varepsilon, \bar{\boldsymbol{\eta}}) = \int_{\Omega_\pm} \frac{1}{\Lambda_\pm^\varepsilon}\left(\bar{\tilde{\mu}}_\pm^\varepsilon - \mathbf{S}_\pm^\varepsilon \cdot \mathbf{e}(\bar{\mathbf{u}}_\pm^\varepsilon)\right)\bar{\tilde{\xi}}_\pm dV_z \tag{18}$$

$$\hat{a}^\varepsilon(\hat{\mathbf{w}}^\varepsilon, \hat{\boldsymbol{\eta}}) = \int_{\Omega_i} \left[\left(\mathbb{C}_i^{\varepsilon,dr}\mathbf{e}_\varepsilon(\hat{\mathbf{u}}^\varepsilon) + \frac{1}{\Lambda_i^\varepsilon}\hat{\tilde{\mu}}^\varepsilon\mathbf{S}_i^\varepsilon\right) \cdot \mathbf{e}_\varepsilon(\hat{\mathbf{v}}) + \mathbf{M}_i^\varepsilon\nabla_\varepsilon\hat{\tilde{\mu}}^\varepsilon \cdot \nabla_\varepsilon\hat{\tilde{\xi}}\right] dV_z \tag{19}$$

$$\hat{b}^\varepsilon(\hat{\mathbf{w}}^\varepsilon, \hat{\boldsymbol{\eta}}) = \int_{\Omega_i} \frac{1}{\Lambda_i^\varepsilon}\left(\hat{\tilde{\mu}}^\varepsilon - \mathbf{S}_i^\varepsilon \cdot \mathbf{e}_\varepsilon(\hat{\mathbf{u}}^\varepsilon)\right)\hat{\tilde{\xi}}\, dV_z \tag{20}$$

$$\bar{l}(\bar{\boldsymbol{\eta}}) = \sum_{k\in\{-,+\}}\int_{\Omega_k} \bar{\mathbf{b}}_k \cdot \bar{\mathbf{v}}_k\, dV_z + \int_{\Gamma_s} \bar{\mathbf{s}} \cdot \bar{\mathbf{v}}\, dS_z - \int_{\Gamma_j} \bar{\bar{j}}\bar{\tilde{\xi}}\, dS_z, \tag{21}$$

where the following notations for a vector field $\hat{\mathbf{f}}$ and a scalar field $\hat{g}$ were introduced

$$\begin{aligned}
&\mathbf{e}_\varepsilon(\hat{\mathbf{f}}) = \frac{1}{\varepsilon}\mathbf{e}_{-1}(\hat{\mathbf{f}}) + \mathbf{e}_0(\hat{\mathbf{f}}),\\
&\nabla_\varepsilon\hat{g} = \frac{1}{\varepsilon}\nabla_{-1}\hat{g} + \nabla_0\hat{g},
\end{aligned} \tag{22}$$

with

$$\begin{aligned}
&\mathbf{e}_{-1}(\hat{\mathbf{f}}) := \mathrm{Sym}(\hat{\mathbf{f}}_{,3} \otimes \mathbf{i}_3),\\
&\mathbf{e}_0 := \mathrm{Sym}(\sum_{\alpha=1}^{2}\hat{\mathbf{f}}_{,\alpha} \otimes \mathbf{i}_\alpha),\\
&\nabla_{-1}\hat{g} := \hat{g}_{,3}\mathbf{i}_3,\\
&\nabla_0\hat{g} := \sum_{\alpha=1}^{2}\hat{g}_{,\alpha}\mathbf{i}_\alpha,
\end{aligned}$$

and $\mathrm{Sym}(\cdot)$ giving the symmetric part of the enclosed tensor $(\cdot)$.

We assume the existence of asymptotic expansions for both the displacement and potential fields in the adherents and in the interphase

$$\begin{aligned}
&\bar{\mathbf{u}}_\pm^\varepsilon = \bar{\mathbf{u}}_\pm^0 + \varepsilon\,\bar{\mathbf{u}}_\pm^1 + o(\varepsilon),\\
&\bar{\tilde{\mu}}_\pm^\varepsilon = \bar{\tilde{\mu}}_\pm^0 + \varepsilon\,\bar{\tilde{\mu}}_\pm^1 + o(\varepsilon),\\
&\hat{\mathbf{u}}^\varepsilon = \hat{\mathbf{u}}^0 + \varepsilon\,\hat{\mathbf{u}}^1 + o(\varepsilon),\\
&\hat{\tilde{\mu}}^\varepsilon = \hat{\tilde{\mu}}^0 + \varepsilon\,\hat{\tilde{\mu}}^1 + o(\varepsilon).
\end{aligned} \tag{23}$$

3.2. Matching of external and internal expansions

As perfect bonding is assumed at the interfaces between the interphase and the adherents, the continuity of the displacement, traction, chemical potential and flux fields is enforced at $S_\pm$. In particular, for the displacement field one has

$$\mathbf{u}^\varepsilon(x_1, x_2, \pm\varepsilon h/2, t) = \hat{\mathbf{u}}^\varepsilon(z_1, z_2, \pm h/2, t) = \bar{\mathbf{u}}_\pm^\varepsilon(z_1, z_2, \pm h/2, t), \tag{24}$$

where $(z_1, z_2) \in S$. Expanding the displacement field in the adherents by a Taylor expansion in the x_3-direction around the limit interface S, one obtains

$$\mathbf{u}^\varepsilon(x_1, x_2, \pm\varepsilon h/2, t) = \mathbf{u}_\pm^\varepsilon(x_1, x_2, 0^\pm, t) \pm \frac{\varepsilon h}{2}\,\mathbf{u}_{\pm,3}^\varepsilon(x_1, x_2, 0^\pm, t) + o(\varepsilon). \tag{25}$$

Substituting into (24) and using the asymptotic expansions (23), one obtains at leading order

$$\mathbf{u}_\pm^0(x_1, x_2, 0^\pm, t) = \hat{\mathbf{u}}^0(z_1, z_2, \pm h/2, t) = \bar{\mathbf{u}}_\pm^0(z_1, z_2, \pm h/2, t), \tag{26}$$

which defines the traces of the limit displacement field on the interface. Denoting by $[\![\hat{f}]\!] := \hat{f}(z_1, z_2, h/2^-) - \hat{f}(z_1, z_2, -h/2^+)$ the inner jump of a field defined in the rescaled interphase, by $[\![\bar{f}]\!] := \bar{f}_+(z_1, z_2, h/2^+) - \bar{f}_-(z_1, z_2, -h/2^-)$ the outer jump between the traces of the adherent fields on the two faces of the rescaled interphase, and by $[\![f]\!] := f_+(x_1, x_2, 0^+) - f_-(x_1, x_2, 0^-)$ the jump of the corresponding limit field across the surface S, one obtains from (26)

$$[\![\mathbf{u}^0]\!] = [\![\bar{\mathbf{u}}^0]\!] = [\![\hat{\mathbf{u}}^0]\!]. \tag{27}$$

A completely analogous argument applies to the chemical potential and to the normal components of the traction and flux. These matching relations allow one to rewrite the asymptotic conditions obtained in the rescaled interphase as transmission conditions posed on the limit interface S, obtained in the limit $\varepsilon \to 0$.

3.3. Scaling regimes and transmission conditions

In the following, the material parameters of the adherents, $\mathbb{C}_\pm^\varepsilon$, $\mathbf{S}_\pm^\varepsilon$, $\Lambda_\pm$ and $\mathbf{M}_\pm^\varepsilon$, will be assumed to be independent of ε, so the notation ε will be dropped for them.

Different scaling assumptions will be adopted for the material parameters of the thin interphase, $\mathbb{C}_i^\varepsilon$, $\mathbf{S}_i^\varepsilon$, Λ_i and $\mathbf{M}_i^\varepsilon$, leading to different limit transmission conditions.

3.3.1. Regime I: interphase with properties comparable to those of the adherents

In this regime, the thin interphase has elastic and chemical properties of the same order as those of the adherents. This corresponds to the case where no scaling is applied to the constitutive parameters:

$$\mathbb{C}_i^\varepsilon = \hat{\mathbb{C}}, \quad \mathbf{S}_i^\varepsilon = \hat{\mathbf{S}}, \quad \Lambda_i^\varepsilon = \hat{\Lambda}, \quad \mathbf{M}_i^\varepsilon = \hat{\mathbf{M}}. \tag{28}$$

Substituting the scaling (28) and the asymptotic expansions (23) into the weak form of the rescaled problem (16) yields a hierarchy of variational problems. Collecting the terms of the same power in ε and equating them to zero, one obtains that the variational equation appearing at order ε^{-1} is

$$\int_{\Omega_i}\left(\hat{\mathbf{K}}^{dr,33}\hat{\mathbf{u}}_{,3}^0 \cdot \hat{\mathbf{v}}_{,3} + \hat{M}_{33}\,\hat{\tilde{\mu}}_{,3}^0\,\hat{\tilde{\xi}}_{,3}\right)dV_z = 0, \tag{29}$$

and that the variational equation appearing at order ε^0 is

$$\begin{aligned}
&\sum_{k\in\{-,+\}}\int_{\Omega_k} \{\left(\mathbb{C}_k^{dr}\mathbf{e}(\bar{\mathbf{u}}_k^0) + \frac{1}{\Lambda_k}\bar{\tilde{\mu}}_k^0\mathbf{S}_k\right) \cdot \mathbf{e}(\bar{\mathbf{v}}_k) + \mathbf{M}_k\nabla\bar{\tilde{\mu}}_k^0 \cdot \nabla\bar{\tilde{\xi}}_k\} dV_z\\
&+ \sum_{k\in\{-,+\}}\int_{\Omega_k} \frac{1}{\Lambda_k}\left(\bar{\tilde{\mu}}_k^0 - \mathbf{S}_k \cdot \mathbf{e}(\bar{\mathbf{u}}_k^0)\right)\bar{\tilde{\xi}}_k dV_z\\
&+ \int_{\Omega_i}\left(\sum_{\alpha=1}^{2}\left(\hat{\mathbf{K}}^{dr,\alpha 3}\hat{\mathbf{u}}_{,3}^0 \cdot \hat{\mathbf{v}}_{,\alpha} + \hat{\mathbf{K}}^{dr,3\alpha}\hat{\mathbf{u}}_{,\alpha}^0 \cdot \hat{\mathbf{v}}_{,3}\right) + \frac{1}{\hat{\Lambda}}\hat{\tilde{\mu}}^0\hat{\mathbf{S}}\mathbf{i}_3 \cdot \hat{\mathbf{v}}_{,3}\right)dV_z
\end{aligned}$$

$$+\int_{\Omega_i}\Big(\hat{\mathbf{K}}^{dr,33}\hat{\mathbf{u}}^1_{,3}\cdot\hat{\mathbf{v}}_{,3}+\hat{M}_{33}\,\hat{\mu}^1_{,3}\,\hat{\xi}_{,3}+\sum_{\alpha=1}^{2}\big(\hat{M}_{3\alpha}\,\hat{\mu}^0_{,\alpha}\,\hat{\xi}_{,3}+\hat{M}_{\alpha 3}\,\hat{\mu}^0_{,3}\,\hat{\xi}_{,\alpha}\big)\Big)dV_z$$
$$=\sum_{k\in\{-,+\}}\int_{\Omega_k}\bar{\mathbf{b}}_k\cdot\bar{\mathbf{v}}_k\,dV_z+\int_{\Gamma_s}\bar{\mathbf{s}}\cdot\bar{\mathbf{v}}\,dS_z-\int_{\Gamma_j}\bar{\jmath}\bar{\xi}\,dS_z, \tag{30}$$

with

$$(\hat{\mathbf{K}}_i)^{jk}_{ih}:=(\mathbb{C}^{dr}_i)_{ijhk}. \tag{31}$$

The two variational equations above are understood to hold for all admissible perturbations in the adherents and the rescaled interphase, provided that the traces are compatible on the surfaces $S_\pm$. Integrating by parts the variational Eq. (29) and applying the localization argument yield the following conditions:

$$\begin{cases}\hat{\mathbf{u}}^0_{,33}=\mathbf{0} & \text{in } \Omega_i,\\ \hat{\mathbf{u}}^0_{,3}=\mathbf{0} & \text{on } S_\pm,\end{cases} \tag{32}$$

and analogous conditions on the potential field at order zero:

$$\begin{cases}\hat{\bar{\mu}}^0_{,33}=0 & \text{in } \Omega_i,\\ \hat{\bar{\mu}}^0_{,3}=0 & \text{on } S_\pm.\end{cases} \tag{33}$$

These conditions imply that $\hat{\mathbf{u}}^0_{,3}$ and $\hat{\bar{\mu}}^0_{,3}$ vanish in Ω_i, so that both $\hat{\mathbf{u}}^0$ and $\hat{\bar{\mu}}^0$ are independent of z_3. This implies

$$[\hat{\mathbf{u}}^0]=\mathbf{0},\quad [\hat{\bar{\mu}}^0]=0, \tag{34}$$

that, by matching these terms with the adherent fields, give

$$[\bar{\mathbf{u}}^0]=\mathbf{0},\quad [\bar{\bar{\mu}}^0]=0. \tag{35}$$

Simplifying the vanishing terms $\hat{\mathbf{u}}^0_{,3}$ and $\hat{\bar{\mu}}^0_{,3}$ in Eq. (30), applying the divergence theorem to the terms defined on $\Omega_\pm$ and localizing give the following equilibrium and balance conditions in the adherents at zeroth order:

$$\begin{aligned}&\operatorname{Div}\bar{\boldsymbol{\sigma}}^0_k+\mathbf{b}_k=\mathbf{0},\quad \text{in } \Omega_k,\qquad k\in\{-,+\}\\ &\dot{\bar{c}}^0_k+\operatorname{Div}\bar{\mathbf{j}}^0_k=0,\quad \text{in } \Omega_k,\qquad k\in\{-,+\},\end{aligned} \tag{36}$$

where

$$\begin{aligned}&\bar{\boldsymbol{\sigma}}^0_k=\mathbb{C}^{dr}_k\mathbf{e}(\bar{\mathbf{u}}^0_k)+\frac{1}{\Lambda_k}\bar{\bar{\mu}}^0_k\mathbf{S}_k\\ &\dot{\bar{c}}^0_k=\frac{1}{\Lambda_k}\dot{\bar{\bar{\mu}}}^0_k-\frac{1}{\Lambda_k}\mathbf{S}_k\cdot\mathbf{e}(\dot{\bar{\mathbf{u}}}^0_k),\\ &\bar{\mathbf{j}}^0_k=-\mathbf{M}_k\nabla\bar{\bar{\mu}}^0_k.\end{aligned} \tag{37}$$

The following conditions emerge in the rescaled adhesive:

$$\hat{\mathbf{u}}^1_{,33}=\mathbf{0}\ \text{ in } \Omega_i, \tag{38}$$

$$\hat{\bar{\mu}}^1_{,33}=0\ \text{ in } \Omega_i, \tag{39}$$

implying that $\hat{\mathbf{u}}^1_{,3}$ and $\hat{\bar{\mu}}^1_{,3}$ are independent of z_3 in Ω_i. On the boundary, the following conditions are found

$$\begin{aligned}&\bar{\boldsymbol{\sigma}}^0\mathbf{n}=\bar{\mathbf{s}},\quad \text{on } \Gamma_s,\\ &\bar{\bar{\mu}}^0=0,\quad \text{on } \Gamma_\mu,\\ &\bar{\mathbf{j}}^0\cdot\mathbf{n}=\check{\jmath},\quad \text{on } \Gamma_j.\end{aligned} \tag{40}$$

Finally, the following conditions are found at the surfaces $S_\pm$:

$$\bar{\boldsymbol{\sigma}}^0_\pm\mathbf{i}_3=\hat{\mathbf{K}}^{dr,3\alpha}\hat{\mathbf{u}}^0_{,\alpha}+\frac{1}{\hat{\Lambda}}\hat{\bar{\mu}}^0\hat{\mathbf{S}}\mathbf{i}_3+\hat{\mathbf{K}}^{dr,33}\hat{\mathbf{u}}^1_{,3}\ \text{ on } S_\pm, \tag{41}$$

$$\bar{\mathbf{j}}^0_\pm\cdot\mathbf{i}_3=-\hat{M}_{3\alpha}\,\hat{\bar{\mu}}^0_{,\alpha}-\hat{M}_{33}\,\hat{\bar{\mu}}^1_{,3}\ \text{ on } S_\pm. \tag{42}$$

Since the right-hand sides are independent of z_3, the corresponding quantities must be continuous across the interphase, yielding

$$[\bar{\boldsymbol{\sigma}}^0\mathbf{i}_3]=\mathbf{0},\quad [\bar{\mathbf{j}}^0\cdot\mathbf{i}_3]=0, \tag{43}$$

which, taken together with (35), constitute the full set of transmission conditions in the rescaled configuration for the present scaling regime.

In conclusion, when the interphase properties are comparable to those of the adherents, it does not affect the overall response, and in the limit of interphase of vanishing thickness the classical perfect interface conditions, both mechanical and chemical, are recovered.

3.3.2. Regime II: interphase with low mobility

In this regime, the thin interphase has properties comparable to those of the adherents, but its mobility is small compared to that of the adherents. This corresponds to the following scalings:

$$\mathbb{C}^\varepsilon_i=\hat{\mathbb{C}},\quad \mathbf{S}^\varepsilon_i=\hat{\mathbf{S}},\quad \Lambda^\varepsilon_i=\hat{\Lambda},\quad \mathbf{M}^\varepsilon_i=\varepsilon\hat{\mathbf{M}}. \tag{44}$$

Substituting the expansions (23) into the rescaled problem (16), using the scaling relation (44), collecting the terms of the same power in ε and equating them to zero, one obtains the following variational equation at order ε^{-1}

$$\int_{\Omega_i}\Big(\hat{\mathbf{K}}^{dr,33}\hat{\mathbf{u}}^0_{,3}\cdot\hat{\mathbf{v}}_{,3}\Big)dV_z=0. \tag{45}$$

The variational equation appearing at order ε^0 is

$$\begin{aligned}&\sum_{k\in\{-,+\}}\int_{\Omega_k}\{\Big(\mathbb{C}^{dr}_k\mathbf{e}(\bar{\mathbf{u}}^0_k)+\frac{1}{\Lambda_k}\bar{\bar{\mu}}^0_k\mathbf{S}_k\Big)\cdot\mathbf{e}(\bar{\mathbf{v}}_k)+\mathbf{M}_k\nabla\bar{\bar{\mu}}^0_k\cdot\nabla\bar{\bar{\xi}}_k\}dV_z\\ &+\sum_{k\in\{-,+\}}\int_{\Omega_k}\frac{1}{\Lambda_k}\Big(\dot{\bar{\bar{\mu}}}^0_k-\mathbf{S}_k\cdot\mathbf{e}(\dot{\bar{\mathbf{u}}}^0_k)\Big)\bar{\bar{\xi}}_k dV_z\\ &+\int_{\Omega_i}\Big(\sum_{\alpha=1}^{2}\big(\hat{\mathbf{K}}^{dr,\alpha 3}\hat{\mathbf{u}}^0_{,3}\cdot\hat{\mathbf{v}}_{,\alpha}+\hat{\mathbf{K}}^{dr,3\alpha}\hat{\mathbf{u}}^0_{,\alpha}\cdot\hat{\mathbf{v}}_{,3}\big)+\frac{1}{\hat{\Lambda}}\hat{\bar{\mu}}^0\hat{\mathbf{S}}\mathbf{i}_3\cdot\hat{\mathbf{v}}_{,3}\Big)dV_z\\ &+\int_{\Omega_i}\Big(\hat{\mathbf{K}}^{dr,33}\hat{\mathbf{u}}^1_{,3}\cdot\hat{\mathbf{v}}_{,3}+\hat{M}_{33}\,\hat{\bar{\mu}}^0_{,3}\,\hat{\xi}_{,3}\Big)dV_z\\ &=\sum_{k\in\{-,+\}}\int_{\Omega_k}\bar{\mathbf{b}}_k\cdot\bar{\mathbf{v}}_k\,dV_z+\int_{\Gamma_s}\bar{\mathbf{s}}\cdot\bar{\mathbf{v}}\,dS_z-\int_{\Gamma_j}\bar{\jmath}\bar{\xi}\,dS_z,\end{aligned} \tag{46}$$

The above variational equations are understood to hold for all admissible perturbations in the adherents and the rescaled interphase, matching at the surfaces $S_\pm$. Integrating by parts the variational equality (45) and applying the localization argument yield that $\hat{\mathbf{u}}^0$ is independent of z_3. By matching this with the adherent fields on $S_\pm$, this result gives

$$[\bar{\mathbf{u}}^0]=\mathbf{0}. \tag{47}$$

Simplifying the vanishing term $\hat{\mathbf{u}}^0_{,3}$ in Eq. (46), applying the divergence theorem to the terms defined on $\Omega_\pm$ and localizing give the equilibrium and balance conditions in the adherents at zeroth order (36), and the boundary conditions (40). The analysis of the variational equation at order ε^0 also reveals the following condition in the rescaled adhesive

$$\begin{aligned}&\hat{\mathbf{K}}^{dr,3\alpha}\hat{\mathbf{u}}^0_{,\alpha 3}+\frac{1}{\hat{\Lambda}}\hat{\bar{\mu}}^0_{,3}\hat{\mathbf{S}}\mathbf{i}_3+\hat{\mathbf{K}}^{dr,33}\hat{\mathbf{u}}^1_{,33}=\mathbf{0}\ \text{ in } \Omega_i,\\ &\hat{\bar{\mu}}^0_{,33}=0\ \text{ in } \Omega_i.\end{aligned} \tag{48}$$

Moreover, the following traction and flux continuity conditions emerge at the surfaces $S_\pm$:

$$\bar{\boldsymbol{\sigma}}^0_\pm\mathbf{i}_3=\hat{\mathbf{K}}^{dr,3\alpha}\hat{\mathbf{u}}^0_{,\alpha}+\frac{1}{\hat{\Lambda}}\hat{\bar{\mu}}^0\hat{\mathbf{S}}\mathbf{i}_3+\hat{\mathbf{K}}^{dr,33}\hat{\mathbf{u}}^1_{,3}\ \text{ on } S_\pm, \tag{49}$$

$$\bar{\mathbf{j}}^0_\pm\cdot\mathbf{i}_3=-\hat{M}_{33}\,\hat{\bar{\mu}}^0_{,3}\ \text{ on } S_\pm. \tag{50}$$

Since the right-hand sides are independent of z_3, in view of Eqs. (48), the corresponding quantities on the left-hand sides must be equal on S_+ and S_-, yielding the continuity of the normal traction and flux across the interface:

$$[\bar{\boldsymbol{\sigma}}^0\mathbf{i}_3]=\mathbf{0},\quad [\bar{\mathbf{j}}^0\cdot\mathbf{i}_3]=0. \tag{51}$$

Finally, let $\bar{\mathbf{j}}^0\cdot\mathbf{i}_3$ denote the trace value of $\bar{\mathbf{j}}^0_\pm\cdot\mathbf{i}_3$ on $S_\pm$. Since $\hat{\bar{\mu}}^0_{,33}$, $\hat{\bar{\mu}}^0_{,3}$ is constant with respect to z_3. Substituting this into the flux continuity condition, integrating with respect to z_3, and matching with the adherent fields on $S_\pm$ yields the final condition

$$\bar{\mathbf{j}}^0\cdot\mathbf{i}_3=-\hat{M}_{33}\frac{[\bar{\bar{\mu}}^0]}{h}. \tag{52}$$

Taken together, conditions (47), (51) and (52) constitute the full set of transmission conditions in the rescaled configuration for the present scaling regime. Since the interphase mobility is low, the chemical flux does not vanish at leading order. Instead, a constitutive relation is obtained linking the continuous normal flux to the jump of chemical potential. This imperfect interface is the diffusive counterpart of the classical Kapitza interface in heat transfer, where a temperature jump is proportional to the heat flux [34].

3.3.3. Regime III: mechanically and chemically weak interphase

In this regime, all constitutive parameters of the thin interphase are assumed to be small, representing a layer in which mechanical, chemical storage, and transport effects are all weak. This leads to the scalings:

$$\mathbb{C}_i^\varepsilon = \varepsilon\,\hat{\mathbb{C}}, \quad \mathbf{S}_i^\varepsilon = \varepsilon\,\hat{\mathbf{S}}, \quad \Lambda_i^\varepsilon = \varepsilon\,\hat{\Lambda}, \quad \mathbf{M}_i^\varepsilon = \varepsilon\hat{\mathbf{M}}. \tag{53}$$

This corresponds to a thin, compliant interphase whose elastic stiffness, chemo-mechanical coupling, and mobility are small compared to those of the adherents.

With the scalings (53), no terms of order ε^{-1} appear. The problem at the lowest order, which is now ε^0, takes the form

$$\int_{\Omega_i} \{\hat{\mathbf{K}}^{dr,33}\hat{\mathbf{u}}^0_{,3}\cdot\hat{\mathbf{v}}_{,3} + \hat{M}_{33}\,\hat{\mu}^0_{,3}\,\hat{\xi}_{,3}\}dV_z$$
$$+ \sum_{k\in\{-,+\}}\int_{\Omega_k}\{\left(\mathbb{C}_k^{dr}\mathbf{e}(\bar{\mathbf{u}}^0_k) + \frac{1}{\Lambda_k}\bar{\mu}^0_k\mathbf{S}_k\right)\cdot\mathbf{e}(\bar{\mathbf{v}}_k) + \mathbf{M}_k\nabla\bar{\mu}^0_k\cdot\nabla\bar{\xi}_k\}dV_z$$
$$+ \sum_{k\in\{-,+\}}\int_{\Omega_k}\frac{1}{\Lambda_k}\left(\dot{\bar{\mu}}^0_k - \mathbf{S}_k\cdot\mathbf{e}(\dot{\bar{\mathbf{u}}}^0_k)\right)\bar{\xi}_k dV_z \tag{54}$$
$$= \sum_{k\in\{-,+\}}\int_{\Omega_k}\bar{\mathbf{b}}_k\cdot\bar{\mathbf{v}}_k\,dV_z + \int_{\Gamma_s}\bar{\mathbf{s}}\cdot\bar{\mathbf{v}}\,dS_z - \int_{\Gamma_j}\bar{\jmath}\bar{\xi}\,dS_z. \tag{55}$$

The first line, containing the interphase terms, is identical to the left-hand side of the variational Eq. (29) from the first scaling case. By integrating by parts with respect to z_3 over the interphase domain Ω_i and localizing,we find that $\hat{\mathbf{u}}^0_{,33} = 0$ and $\hat{\mu}^0_{,33} = 0$ in Ω_i, so that $\hat{\mathbf{u}}^0_{,3}$ and $\hat{\mu}^0_{,3}$ are independent of z_3. From the remaining terms in the ε^0 variational equation, using the divergence theorem for the term defined in the adherents and localizing, we recover the equilibrium and balance conditions (36) and the boundary conditions (40). Finally, the analysis yields the following set of conditions on $S_\pm$:

$$\bar{\boldsymbol{\sigma}}^0_\pm\mathbf{i}_3 = \hat{\mathbf{K}}^{dr,33}\hat{\mathbf{u}}^0_{,3} \quad \text{on } S_\pm,$$
$$\bar{\mathbf{j}}^0_\pm\cdot\mathbf{i}_3 = -\hat{M}_{33}\,\hat{\mu}^0_{,3} \quad \text{on } S_\pm. \tag{56}$$

Using the fact that $\hat{\mathbf{u}}^0_{,3}$ and $\hat{\mu}^0_{,3}$ are independent of z_3, together with the matching conditions at $S_\pm$, yields the following continuity conditions:

$$[\bar{\boldsymbol{\sigma}}^0\mathbf{i}_3] = \mathbf{0}, \tag{57}$$
$$[\bar{\mathbf{j}}^0\cdot\mathbf{i}_3] = 0. \tag{58}$$

Then, by integrating the relations (56) through the thickness and using the matching conditions, we obtain the jump conditions:

$$\bar{\boldsymbol{\sigma}}^0\mathbf{i}_3 = \hat{\mathbf{K}}^{dr,33}\frac{[\bar{\mathbf{u}}^0]}{h}, \tag{59}$$
$$\bar{\mathbf{j}}^0\cdot\mathbf{i}_3 = -\hat{M}_{33}\frac{[\bar{\mu}^0]}{h}. \tag{60}$$

These conditions are chemo-mechanically decoupled. This structure is analogous to that obtained for soft thermo-elastic interfaces at zeroth order [17], where the mechanical spring-type law is independent of the temperature jump and the thermal resistance law is independent of the displacement jump.

3.3.4. Regime IV: soft interphase with mobility comparable to that of the adherents

In this regime, the thin interphase is mechanically soft, with weak chemo-mechanical coupling and low storage capacity, while its mobility is comparable to that of the adherents. This leads to the scalings:

$$\mathbb{C}_i^\varepsilon = \varepsilon\,\hat{\mathbb{C}}, \quad \mathbf{S}_i^\varepsilon = \varepsilon\,\hat{\mathbf{S}}, \quad \Lambda_i^\varepsilon = \varepsilon\,\hat{\Lambda}, \quad \mathbf{M}_i^\varepsilon = \hat{\mathbf{M}}. \tag{61}$$

Substituting the expansions (23) into the rescaled problem (16), using the scalings (61), collecting the terms of the same power in ε and equating them to zero, gives the following variational equation at order ε^{-1} :

$$\int_{\Omega_i}\left(\hat{M}_{33}\,\hat{\mu}^0_{,3}\,\hat{\xi}_{,3}\right)dV_z = 0, \tag{62}$$

and the following variational equation at order ε^0 :

$$\sum_{k\in\{-,+\}}\int_{\Omega_k}\{\left(\mathbb{C}_k^{dr}\mathbf{e}(\bar{\mathbf{u}}^0_k) + \frac{1}{\Lambda_k}\bar{\mu}^0_k\mathbf{S}_k\right)\cdot\mathbf{e}(\bar{\mathbf{v}}_k) + \mathbf{M}_k\nabla\bar{\mu}^0_k\cdot\nabla\bar{\xi}_k\}dV_z$$
$$+ \sum_{k\in\{-,+\}}\int_{\Omega_k}\frac{1}{\Lambda_k}\left(\dot{\bar{\mu}}^0_k - \mathbf{S}_k\cdot\mathbf{e}(\dot{\bar{\mathbf{u}}}^0_k)\right)\bar{\xi}_k dV_z + \int_{\Omega_i}\frac{1}{\hat{\Lambda}}\left(\dot{\hat{\mu}}^0 - \hat{\mathbf{S}}\mathbf{i}_3\cdot\dot{\hat{\mathbf{u}}}^0_{,3}\right)\hat{\xi}dV_z$$
$$+ \int_{\Omega_i}\left(\hat{\mathbf{K}}^{dr,33}\hat{\mathbf{u}}^0_{,3}\cdot\hat{\mathbf{v}}_{,3} + \frac{1}{\hat{\Lambda}}\hat{\mu}^0\hat{\mathbf{S}}\mathbf{i}_3\cdot\hat{\mathbf{v}}_{,3}\right)dV_z$$
$$+ \int_{\Omega_i}\left(\hat{M}_{33}\,\hat{\mu}^1_{,3}\,\hat{\xi}_{,3} + \sum_{\alpha=1}^{2}\left(\hat{M}_{3\alpha}\,\hat{\mu}^0_{,\alpha}\,\hat{\xi}_{,3} + \hat{M}_{\alpha 3}\,\hat{\mu}^0_{,3}\,\hat{\xi}_{,\alpha}\right)\right)dV_z$$
$$= \sum_{k\in\{-,+\}}\int_{\Omega_k}\bar{\mathbf{b}}_k\cdot\bar{\mathbf{v}}_k\,dV_z + \int_{\Gamma_s}\bar{\mathbf{s}}\cdot\bar{\mathbf{v}}\,dS_z - \int_{\Gamma_j}\bar{\jmath}\bar{\xi}\,dS_z. \tag{63}$$

Integrating by parts the variational equality (62) and applying the localization argument give the conditions (33), which in turn yield the continuity condition

$$[\bar{\mu}^0] = 0. \tag{64}$$

From the remaining terms in the ε^0 variational Eq. (63), using the divergence theorem for the term defined in the adherents and localizing, we recover the equilibrium and balance conditions (36) and the boundary conditions (40). Finally, the analysis yields the following conditions in Ω_i :

$$\hat{\mathbf{K}}^{dr,33}\hat{\mathbf{u}}^0_{,33} = \mathbf{0} \quad \text{in } \Omega_i,$$
$$\hat{M}_{33}\,\hat{\mu}^1_{,33} + \sum_{\alpha=1}^{2}\left(\hat{M}_{3\alpha}\,\hat{\mu}^0_{,\alpha 3} + \hat{M}_{\alpha 3}\,\hat{\mu}^0_{,33}\right) + \frac{1}{\hat{\Lambda}}\left(\hat{\mathbf{S}}\mathbf{i}_3\cdot\dot{\hat{\mathbf{u}}}^0_{,3} - \dot{\hat{\mu}}^0\right) = 0 \quad \text{in } \Omega_i. \tag{65}$$

Moreover, the following traction and flux continuity conditions emerge at the surfaces $S_\pm$:

$$\bar{\boldsymbol{\sigma}}^0_\pm\mathbf{i}_3 = \hat{\mathbf{K}}^{dr,33}\hat{\mathbf{u}}^0_{,3} + \frac{1}{\hat{\Lambda}}\hat{\mu}^0\hat{\mathbf{S}}\mathbf{i}_3, \quad \text{on } S_\pm, \tag{66}$$
$$\bar{\mathbf{j}}^0_\pm\cdot\mathbf{i}_3 = -\hat{M}_{33}\,\hat{\mu}^1_{,3} - \sum_{\alpha=1}^{2}\hat{M}_{3\alpha}\,\hat{\mu}^0_{,\alpha} \quad \text{on } S_\pm. \tag{67}$$

Using the fact that $\hat{\mu}^0$ is independent of z_3, and $\hat{\mathbf{u}}^0_{,3}$ is constant, cf. (33) and the first condition in (65), one obtains that $\bar{\boldsymbol{\sigma}}^0_\pm\mathbf{i}_3$ are equal on $S_\pm$, a result that yields the continuity of the traction vector

$$[\bar{\boldsymbol{\sigma}}^0\mathbf{i}_3] = \mathbf{0}. \tag{68}$$

Moreover, in view of (64) one obtains that

$$\bar{\boldsymbol{\sigma}}^0\mathbf{i}_3 = \hat{\mathbf{K}}^{dr,33}\frac{[\hat{\mathbf{u}}^0]}{h} + \frac{1}{\hat{\Lambda}}\hat{\mu}^0\hat{\mathbf{S}}\mathbf{i}_3 \tag{69}$$

Integrating the second equation in (65) across the thickness and using the flux expressions (67) gives

$$[\bar{\mathbf{j}}^0\cdot\mathbf{i}_3] = \frac{1}{\hat{\Lambda}}\left((\hat{\mathbf{S}}\mathbf{i}_3)\cdot[\dot{\mathbf{u}}] - h\,\dot{\hat{\mu}}^0\right), \tag{70}$$

Eqs. (64), (68), (69), and (70) constitute the full set of transmission conditions for the present scaling regime. In this case, the mechanical and chemical interface laws are coupled, making this the most general regime obtained in the analysis.

Notably, the right-hand side of (70) can be viewed as the time-derivative of the opposite of the leading-order concentration variation in the interphase. This can also be interpreted as a surface excess concentration. In this viewpoint, the jump of the normal chemical flux expresses a surface mass balance at the limit interface. In this sense, the resulting transmission condition represents a mass balance at the interface, in contrast with the constitutive flux laws obtained in the previous scaling regimes, cf. (52).

Table 1
Limit interface laws posed on the interface S, obtained from the asymptotic analysis under different scalings of the interphase parameters.

Regime	$\mathbb{C}_i^\varepsilon, \mathbf{S}_i^\varepsilon, \Lambda_i^\varepsilon$	$\mathbf{M}_i^\varepsilon$	Transmission conditions	
			Mechanical	Chemical
I	$O(1)$	$O(1)$	**Perfect** $[\![\mathbf{u}]\!] = 0$ $[\![\boldsymbol{\sigma}\mathbf{i}_3]\!] = 0$	**Perfect** $[\![\tilde{\mu}]\!] = 0$ $[\![\mathbf{j}\cdot\mathbf{i}_3]\!] = 0$
II	$O(1)$	$O(\varepsilon)$	**Perfect** $[\![\mathbf{u}]\!] = 0$ $[\![\boldsymbol{\sigma}\mathbf{i}_3]\!] = 0$	**Resistive** $[\![\mathbf{j}\cdot\mathbf{i}_3]\!] = 0$ $\mathbf{j}\cdot\mathbf{i}_3 = -M^\varepsilon_{i,33}\dfrac{[\![\tilde{\mu}]\!]}{h^\varepsilon}$
III	$O(\varepsilon)$	$O(\varepsilon)$	**Imperfect** $[\![\boldsymbol{\sigma}\mathbf{i}_3]\!] = 0$ $\boldsymbol{\sigma}\mathbf{i}_3 = (\mathbf{K}_i^\varepsilon)^{dr,33}\dfrac{[\![\mathbf{u}]\!]}{h^\varepsilon}$	**Resistive** $[\![\mathbf{j}\cdot\mathbf{i}_3]\!] = 0$ $\mathbf{j}\cdot\mathbf{i}_3 = -M^\varepsilon_{i,33}\dfrac{[\![\tilde{\mu}]\!]}{h^\varepsilon}$
IV	$O(\varepsilon)$	$O(1)$	**Imperfect** $[\![\boldsymbol{\sigma}\mathbf{i}_3]\!] = 0$ $\boldsymbol{\sigma}\mathbf{i}_3 = (\mathbf{K}_i^\varepsilon)^{dr,33}\dfrac{[\![\mathbf{u}]\!]}{h^\varepsilon} + \dfrac{\mathbf{S}_i^\varepsilon\mathbf{i}_3}{\Lambda_i^\varepsilon}\,\tilde{\mu}$	**Coupled** $[\![\tilde{\mu}]\!] = 0$ $[\![\mathbf{j}\cdot\mathbf{i}_3]\!] = \dfrac{\mathbf{S}_i^\varepsilon\mathbf{i}_3}{\Lambda_i^\varepsilon}\cdot[\![\dot{\mathbf{u}}]\!] - \dfrac{h^\varepsilon}{\Lambda_i^\varepsilon}\,\dot{\tilde{\mu}}$

4. Summary of results

The asymptotic analysis presented so far leads to a reduced problem posed in the adherent domains $\Omega_\pm$, coupled through effective transmission conditions on the interface S. At leading order, the fields in the adherents satisfy the equilibrium and mass balance Eqs. (36), together with the constitutive relations (37). These equations are identical in structure to the original ones, but are now supplemented by interface laws that incorporate the effect of the vanishingly thin interphase.

The interface laws obtained from the previous asymptotic analysis are summarized in Table 1. All fields appearing in the table are leading-order fields in the limit configuration as the interphase thickness tends to zero. The superscript 0 is omitted for brevity. When a quantity is continuous across the interface, the table reports the corresponding interfacial trace on S. The interface laws are posed on the interface S and involve the jumps $[\![\cdot]\!]$ of the corresponding fields, the small thickness $h^\varepsilon = \varepsilon h$ of the interphase and its original, unrescaled material parameters. In addition to the classical perfect and resistive behaviors, the asymptotic analysis revealed that coupled chemo-mechanical effects may arise at the interface. These four regimes provide a unified interpretation of classical and non-classical interface laws within a single asymptotic framework.

The four regimes listed in Table 1 have a clear physical interpretation. Regime I corresponds to an interphase whose elastic, chemical, and transport properties remain comparable with those of the adherents. As a consequence, the leading-order effect of the vanishing layer disappears and the classical perfect interface is recovered. Regime II describes an interphase with standard mechanical stiffness but reduced mobility. Since the mobility is small, a finite resistance to mass transport appears, while mechanical transmission remains perfect. Regime III corresponds to a soft, low-mobility interphase, such as a compliant adhesive layer with limited transport. Since its constitutive and transport parameters are small, the interface behaves as a soft layer, resulting in uncoupled spring-type mechanical and resistive chemical laws.

Regime IV is less standard. It describes a soft but chemically active interphase, for example a gel-like, swelling, or functional coating layer, in which mechanical compliance, chemical storage, and species exchange remain coupled in the limit. The interphase is mechanically soft but has finite mobility, leading to a coupled interface law in which the jump of the displacement, the interfacial potential, and the jump of normal flux are linked. This feature distinguishes Regime IV from the previous three regimes. In Regimes I–III, the normal flux is continuous across the interface, and the interface only transmits mass transport in Regime I or resists it in Regimes II and III. In Regime IV, instead, the jump of normal flux does not vanish and it is balanced by the rate of change of an interfacial excess amount. The limit interface therefore acts as an exchange very thin layer, rather than as a purely transmissive or resistive surface. The physical consequences of Regime IV, including its interpretation in terms of an interfacial excess amount, will be illustrated in the following example.

5. An illustrative example

Consider a one-dimensional composite bar composed of two identical chemoelastic adherents occupying the intervals $(-L, 0)$ and $(0, L)$, connected at $x = 0$ through one of the interface laws derived in the previous sections, as represented in Fig. 1. The external boundaries are assumed chemically sealed, i.e. $\tilde{\mu}'(\pm L, t) = 0$, $t > 0$, where a prime denotes differentiation with respect to x. A time-dependent tensile stress $\sigma(L, t) = q(t)$, $t > 0$, with $q(0) = 0$, is prescribed at the right-hand extremity of the bar, while the left-hand extremity is kept fixed, i.e. $u_-(-L, t) = 0$, $t > 0$. The initial conditions are taken as $u_\pm(x, 0) = 0$, $\tilde{\mu}_\pm(x, 0) = 0$, $x \in (-L, L)$. The following constitutive equations hold for each adherent part:

$$\sigma_\pm = E^{dr}u'_\pm + \frac{s}{\Lambda}\tilde{\mu}_\pm, \tag{71}$$

$$\tilde{c}_\pm = \frac{1}{\Lambda}\tilde{\mu}_\pm - \frac{s}{\Lambda}u'_\pm, \tag{72}$$

$$j_\pm = -m\tilde{\mu}'_\pm, \tag{73}$$

where $E^{dr} = E - s^2/\Lambda$. In each adherent part, the local balance of linear momentum and the mass balance read as follows:

$$\left(E^{dr}u'_\pm + \frac{s}{\Lambda}\tilde{\mu}_\pm\right)' = 0, \tag{74}$$

$$\Lambda m\tilde{\mu}''_\pm - \frac{E}{E^{dr}}\dot{\tilde{\mu}}_\pm = -\frac{s}{E^{dr}}\dot{q}(t). \tag{75}$$

For the first three interface laws listed in Table 1, a solution of the chemoelastic problem is given by the following spatially uniform chemical potential, vanishing chemical flux and piecewise linear displacement fields:

$$\tilde{\mu}_\pm = \frac{s}{E}q(t), \tag{76}$$

$$j_\pm = 0, \tag{77}$$

$$u_- = \frac{q(t)}{E}(x + L), \tag{78}$$

$$u_+ = \frac{q(t)}{E}(x + L) + [\![u]\!], \tag{79}$$

$$\sigma_\pm = q(t), \tag{80}$$

with $[\![u]\!]$ the displacement jump at $x = 0$. Imposing the interface laws I and II, one has $[\![u]\!] = 0$. Imposing the interface law III, one finds $[\![u]\!] = h^\varepsilon q(t)/k_i^\varepsilon$. Thus, under the present loading conditions, no diffusion takes place. The difference between the regime given by the

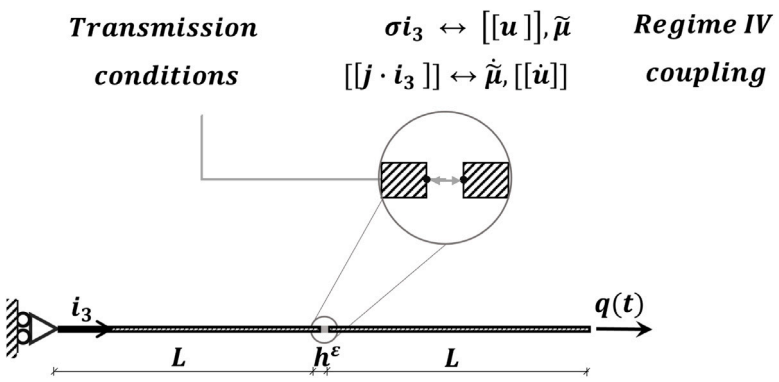


Fig. 1. One-dimensional composite with chemically sealed external boundaries subjected to a time-dependent loading $q(t)$. The composite consists of two identical adherents of length L, occupying the intervals $(-L, 0)$ and $(0, L)$, connected at $x = 0$ through one of the four transmission conditions listed in Table 1. The inset schematically illustrates the coupled transmission law of Regime IV, relating the traction vector σi_3 to the displacement jump $[\![u]\!]$ and the interfacial chemical potential $\tilde{\mu}$, and the flux jump $[\![j \cdot i_3]\!]$ to $\dot{\tilde{\mu}}$ and $[\![\dot{u}]\!]$.

transmission conditions I or II, and the regime given by the transmission conditions III arises only through the displacement jump condition at the interface.

The macroscopic response of the composite bar is given in terms of the macroscopic strain, defined as

$$\epsilon(t) = \frac{u_+(L,t) - u_-(-L,t)}{2L}. \tag{81}$$

Using (79), this can be written as

$$\epsilon(t) = \frac{q(t)}{E} + \frac{[\![u]\!]}{2L}, \tag{82}$$

where $[\![u]\!]$ denotes the displacement jump at the interface. For the first two interface laws, one has $[\![u]\!] = 0$, so that the classical relation $\epsilon = q/E$ is obtained. For the third interface law, the jump is proportional to the applied stress, leading to the following stress–strain response:

$$q = \frac{\epsilon}{\left(\frac{1}{E} + \xi \frac{1}{(k_i^\varepsilon)^{dr}}\right)}, \tag{83}$$

where $\xi := h^\epsilon/(2L)$ is the volume fraction of the interphase material, and $(k_i^\varepsilon)^{dr}$ is the drained mechanical stiffness coefficient of the thin interphase. The result (83) corresponds to the classical series combination of bulk and interfacial compliance.

The fourth interface law yields a qualitatively different chemo-mechanical response of the composite bar. Introducing the decomposition

$$\tilde{\mu}_\pm(x,t) = \frac{s}{E} q(t) + \theta_\pm(x,t), \tag{84}$$

the mass balance equations in the two adherents reduce to

$$\dot{\theta}_\pm - D\theta''_\pm = 0, \qquad D := \frac{\Lambda m E^{dr}}{E}. \tag{85}$$

Since $q(0) = 0$ and $\tilde{\mu}_\pm(x,0) = 0$, the initial condition for the perturbation is

$$\theta_-(x,0) = 0, \qquad \theta_+(x,0) = 0. \tag{86}$$

The external sealed-boundary conditions impose

$$\theta'_-(-L,t) = 0, \qquad \theta'_+(L,t) = 0, \qquad t > 0, \tag{87}$$

while the continuity of the potential at the interface in $x = 0$ prescribes

$$\theta_+(0,t) = \theta_-(0,t), \qquad t > 0. \tag{88}$$

The remaining interface conditions are

$$q(t) = \frac{(k_i^\varepsilon)^{dr}}{h^\epsilon} [\![u]\!](t) + \frac{s_i^\varepsilon}{\Lambda_i^\varepsilon} \tilde{\mu}(0,t), \qquad t > 0, \tag{89}$$

$$[\![j]\!](t) = \frac{s_i^\varepsilon}{\Lambda_i^\varepsilon} [\![\dot{u}]\!](t) - \frac{h^\varepsilon}{\Lambda_i^\varepsilon} \dot{\tilde{\mu}}(0,t), \qquad t > 0. \tag{90}$$

Eliminating $[\![u]\!]$ yields

$$[\![j]\!](t) = \alpha_i^\varepsilon \, \dot{q}(t) - \beta_i^\varepsilon \, \dot{\tilde{\mu}}(0,t), \qquad t > 0, \tag{91}$$

with

$$\alpha_i^\varepsilon := \frac{s_i^\varepsilon h^\varepsilon}{\Lambda_i^\varepsilon (k_i^\varepsilon)^{dr}}, \qquad \beta_i^\varepsilon := \frac{h^\varepsilon}{\Lambda_i^\varepsilon} \left(1 + \frac{(s_i^\varepsilon)^2}{\Lambda_i^\varepsilon (k_i^\varepsilon)^{dr}}\right). \tag{92}$$

Using (84), this becomes

$$[\![j]\!](t) = \left(\alpha_i^\varepsilon - \beta_i^\varepsilon \frac{s}{E}\right) \dot{q}(t) - \beta_i^\varepsilon \dot{\theta}(0,t), \qquad t > 0, \tag{93}$$

which, in view of $j_\pm = -m\tilde{\mu}'_\pm = -m\theta'_\pm$, gives

$$\theta'_+(0,t) - \theta'_-(0,t) = \frac{1}{m}\left(\beta_i^\varepsilon \frac{s}{E} - \alpha_i^\varepsilon\right)\dot{q}(t) + \frac{\beta_i^\varepsilon}{m}\dot{\theta}(0,t), \qquad t > 0, \tag{94}$$

where $\dot{\theta}(0,t)$ denotes the interfacial trace of $\dot{\theta}_-(0,t)$ and $\dot{\theta}_+(0,t)$, which coincide by continuity.

Therefore, the perturbation fields $\theta_\pm$ solve the diffusion problems (85) in the two adherents, supplemented by the initial condition (86), the sealed external boundary conditions (87), the continuity condition (88), and the time-dependent interface condition (94). This structure, which couples a diffusion problem with an evolution equation for the interfacial value, is the main distinction between interface law IV and the other three regimes. Indeed, for the latter ones, the chemical interface condition reduces to

$$\theta'_-(0,t) = \theta'_+(0,t). \tag{95}$$

Together with the initial condition and the sealed external boundaries, this condition gives the null perturbation field $\theta_\pm(x,t) = 0$. Accordingly, no diffusion process takes place in the adherents and the spatially uniform chemical potential (76) is recovered.

Notably, for interface law IV, the flux is no longer continuous across the interface, cf. (93). This implies that, although the external boundaries are sealed, the amount of chemical species contained in the adherents is not conserved. Indeed, integrating the mass balance over the two adherents and using the sealed-boundary conditions (87) gives

$$\frac{d}{dt}\int_{-L}^{L} \tilde{c}(x,t)\,dx = j_+(0,t) - j_-(0,t) = [\![j]\!](t). \tag{96}$$

Using (91), this becomes

$$\frac{d}{dt}\int_{-L}^{L} \tilde{c}(x,t)\,dx = \alpha_i^\varepsilon \dot{q}(t) - \beta_i^\varepsilon \dot{\tilde{\mu}}(0,t). \tag{97}$$

Equivalently,

$$\frac{d}{dt}\left[\int_{-L}^{L} \tilde{c}(x,t)\,dx + \tilde{c}_S(t)\right] = 0, \tag{98}$$

Table 2
Geometric, material, and loading parameters used in the numerical application.

Quantity	Symbol	Value	Unit
Adherents			
Bar half-length	L	1	mm
Elastic modulus	E	1	MPa
Chemical modulus	Λ	1	MPa m^6/mol^2
Coupling coefficient	s	−0.7	MPa m^3/mol
Drained modulus	E^{dr}	0.51	MPa
Mobility	m	5.0×10^{-18}	mol^2/(Pa m^4 s)
Diffusivity	D	2.55×10^{-12}	m^2/s
Interphase			
Thickness	h^ε	0.05	mm
Drained stiffness	$(k_i^\varepsilon)^{dr}$	0.08	MPa
Chemical modulus	Λ_i^ε	0.06	MPa m^6/mol^2
Coupling coefficient	s_i^ε	−0.06	MPa m^3/mol
Interface parameter	α_i^ε	-6.25×10^{-10}	mol/(Pa m^2)
Interface parameter	β_i^ε	1.46×10^{-9}	mol^2/(Pa m^5)
Loading			
Characteristic diffusion time	τ_D	3.92×10^5	s
Characteristic loading time	τ_q	$\{0.01,\ 0.1,\ 1\}\times\tau_D$	–
Asymptotic stress	q_∞	0.01	MPa
Loading rate	q_∞/τ_q	$2.55,\ 2.55\times10^{-1},\ 2.55\times10^{-2}$	Pa/s

with $\tilde{c}_S(t) := \beta_i^\varepsilon\tilde{\mu}(0,t) - \alpha_i^\varepsilon q(t)$. The relation shows that mass conservation is only recovered only if the interfacial contribution $\tilde{c}_S$ is included. The quantity $\tilde{c}_S$ can be interpreted as the interfacial excess amount per unit area associated with the limit interface. This shows that the limit interface may exchange chemical species with the adherents, even though the external boundaries are chemically sealed. The sign of the exchange is determined by the rate of change of the term $\tilde{c}_S$: a decrease of this quantity corresponds to a release of chemical species from the limit interface to the adherents, whereas an increase corresponds to the absorption of chemical species by the interface.

This interpretation is analogous to the classical concept of surface excess, where the effect of a thin transition region is assigned to an idealized dividing surface [26,35]. Here, the dividing surface is the limit interface S, and $\tilde{c}_S$ is the amount of species per unit area associated with the vanishing interphase. Notably, $\tilde{c}_S$ is not introduced as an additional surface variable, but it follows from the asymptotic species balance. Thus, the non-zero flux jump in Regime IV describes species exchange between the interface and the adherents.

For a numerical application, symmetry allows the problem to be solved on the right half-bar $x\in(0,L)$, where $x=0$ is the interface and $x=L$ the sealed external boundary. With $\theta(x,t)=\theta_+(x,t)=\theta_-(-x,t)$, one obtains

$$\dot{\theta} - D\theta'' = 0, \qquad 0<x<L, \tag{99}$$

$$\theta'(L,t)=0, \qquad \beta_i^\varepsilon\dot{\theta}(0,t) - 2m\theta'(0,t) = \left(\alpha_i^\varepsilon - \beta_i^\varepsilon\frac{s}{E}\right)\dot{q}(t). \tag{100}$$

Since the latter interface condition contains the time derivative of the interfacial value $\theta(0,t)$, the method of lines naturally accommodates the coupled PDE/ODE structure by providing the spatial discretization [36]. The resulting system of ordinary differential equations is then integrated in time using MATLAB's `ode15s` solver [37]. After numerically estimating the function $\theta(x,t)$, the chemical potential can be evaluated using Eq. (84). Then, the strain and concentration can be calculated using constitutive Eqs. (71) and (72). In particular, by combining Eqs. (84), (71), (72), and (80), one can show that the concentrations in the adherents, $\tilde{c}_\pm$, are proportional to $\theta_\pm$ as follows:

$$\tilde{c}_\pm = \frac{E}{\Lambda E^{dr}}\theta_\pm. \tag{101}$$

In the numerical application, the following exponential loading history is considered:

$$q(t) = q_\infty\left(1-e^{-t/\tau_q}\right), \tag{102}$$

which represents a monotonically increasing load approaching the plateau value q_∞.

To highlight the qualitative differences between the time-dependent chemomechanical responses induced by this loading history, the geometric, material, and loading parameters listed in Table 2 are adopted. These values are not intended to model a specific composite. Rather, they are taken to provide a representative framework for comparing the responses associated with the four interface laws. In particular, they were selected so as to produce a mechanically soft interphase, a slow diffusion process on the macroscopic length scale, and a measurable chemo-mechanical coupling, while preserving the positivity of the drained moduli. The mobility and length scale lead to a characteristic diffusion time representative of slow transport in soft or polymeric materials. The loading times are then chosen as fractions or multiples of this diffusion time, in order to compare fast, intermediate, and slow loading conditions with respect to the diffusion process.

The half-length $L = 1$ mm is selected so that, for the chosen diffusivity, the characteristic diffusion time $\tau_D := L^2/D$ is of the order of a few days. The coupling coefficients are chosen so that the drained moduli of both the adherents and the interphase are positive. The value of the asymptotic stress is chosen so that the resulting strains remain within the small-strain range assumed in the formulation. Different loading times τ_q are considered to assess the effect of the loading rate on the chemo-mechanical response of the composite bar.

Fig. 2 illustrates the chemical response of the composite bar. As discussed above, interface laws I–III lead to the trivial perturbation field $\theta_\pm = 0$, and are therefore represented by the horizontal dotted line. Law IV induces non-zero perturbation fields $\theta_\pm$. Panel (a) of Fig. 2 shows the profiles of $\theta_\pm$ at selected times for $\tau_q = 0.1\tau_D$. The perturbation, initially localized near the interface, progressively expands into the adherents as diffusion takes place.

Since $\theta_\pm$ are proportional to the corresponding concentration perturbations, cf. (101), the same profiles also describe the evolution of the concentration fields up to a constant factor. Panel (b) of Fig. 2 shows the interfacial value $\theta(0,t)$ for different loading times. The largest peak is obtained for the fastest loading, namely, for $\tau_q = 0.01\tau_D$. However, this does not indicate a faster diffusion process, as the diffusivity remains constant. Rather, it shows that the chemical perturbation acts on a timescale much shorter than the diffusion time. Thus, the perturbation initially accumulates near the interface and later relaxes by diffusion. When the loading rate is slower, the perturbation does not accumulate near the interface because diffusion redistributes it. This behavior highlights the rate dependence of the chemical response associated with transmission regime IV.

The mechanical response of the composite bar is shown in Fig. 3. To illustrate the effect of the interface, panel (a) of Fig. 3 shows the quantity

$$\epsilon(t) - \frac{q(t)}{E} = \frac{[\![u]\!](t)}{2L}, \tag{103}$$

which represents the interfacial contribution to the macroscopic strain, or equivalently the displacement jump normalized by the total length of the bar. For laws I–II this contribution vanishes, consistent with the perfect mechanical transmission condition. For law III, it is purely mechanical and proportional to the applied stress, see the discussion after (80). For law IV, instead, the interfacial contribution also depends on the chemical perturbation at the interface. For fast loading, the chemical perturbation cannot redistribute quickly, so the initial response is mainly determined by the mechanical stiffness of the interface, resulting in a peak in the curve. The subsequent evolution of the interfacial chemical potential relaxes this response. For slower loading, the chemical field evolves as the load is applied, resulting in a more gradual interfacial response.

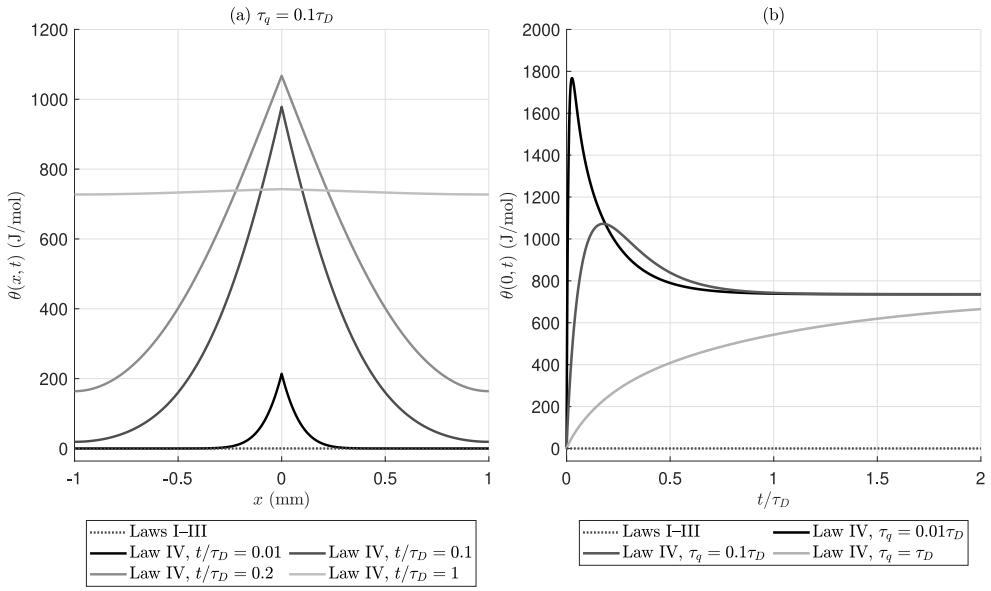


Fig. 2. Chemical response of the composite bar for the four interfacial transmission regimes. (a) Profiles of the perturbation field $\theta(x,t)$ at selected times. (b) Time evolution of the interfacial value $\theta(0,t)$ for different loading times τ_q.

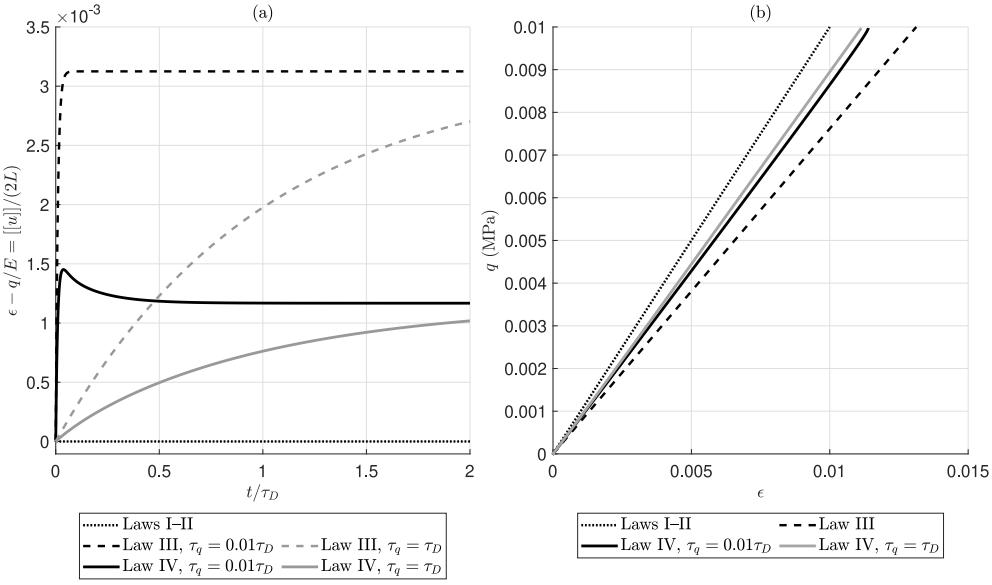


Fig. 3. Mechanical response of the composite bar for the four interfacial transmission regimes. (a) Interfacial contribution to the macroscopic strain, $\epsilon - q/E = [\![u]\!]/(2L)$, for different loading times. (b) Macroscopic stress–strain responses.

Panel (b) of Fig. 3 shows the macroscopic stress–strain curves. Laws I–II and law III give linear and rate independent responses, since the corresponding displacement jump is either zero or linearly proportional to the applied stress, cf. (83). For law IV the response depends on the loading time τ_q, because the displacement jump is coupled with the evolving interfacial chemical potential. The curve is therefore not determined only by the instantaneous value of the applied stress, but also by the transient chemical state of the interface. The macroscopic response for law IV is shown for two different loading times, τ_q. The comparison between the two curves shows that this macroscopic response is rate-dependent, which is consistent with the chemical response shown in the panel (b) of Fig. 2 and previously discussed.

The example shows that interface law IV introduces an intrinsic interfacial timescale. Although the adherents are subjected to a spatially uniform tensile stress, the coupling between the displacement jump rate and the interfacial chemical potential rate generates a transient redistribution of chemical potential. This effect is absent in the first three regimes, during which the chemical response remains uniform and no diffusion process occurs. In conclusion, interface law IV accurately describes the delayed chemo-mechanical response of the original thin interphase, whose internal evolutionary behavior is preserved in the limit interface model.

6. Conclusion

In this work, an asymptotic analysis of a thin chemoelastic interphase has been carried out to derive effective interface models. Particular attention has been devoted to the role of the scaling of the constitutive parameters, which determines the relative importance of elasticity, diffusion, chemical storage, and chemo-mechanical coupling in the limit model.

The results show that different scaling regimes lead to distinct transmission conditions, as summarized in Table 1. The corresponding interface laws range from classical perfect conditions to imperfect mechanical laws, chemical resistance laws, and coupled chemo-mechanical transmission conditions. The asymptotic procedure therefore does not introduce interface models arbitrarily, but identifies the models associated with specific interplay between the constitutive properties of the interphase and its vanishing thickness. In this sense, scaling acts as a selection principle for admissible interface behaviors.

The analysis also illustrates the versatility of the method of asymptotic expansions for multiphysics interface problems. Starting from a single three-dimensional chemoelastic description, different limit interface models are obtained within a unified framework. Moreover by eliminating the small geometric scale associated with the interphase thickness, these models may be used in combination with finite element discretizations of the adherents to avoid the explicit meshing of very thin layers and thereby reduce the computational cost of simulations.

The one-dimensional example of a composite bar under traction and chemically sealed boundary conditions illustrates the physical meaning of the four regimes. Under the considered loading conditions, Laws I and II give the response of the perfectly bonded composite, while Law III add a purely mechanical interfacial compliance to the macroscopic response. Law IV produces a different behavior: the mechanical jump is coupled with the chemical state of the interface, and a transient chemical perturbation is generated near the interface. This evolving chemical state affects the macroscopic strain and makes the interfacial contribution rate-dependent. The corresponding interface condition can be interpreted in terms of a surface excess contribution, in analogy with classical concepts from physical chemistry [26]. In the present setting, this chemo-mechanical contribution is not postulated *a priori*, but it is a result of the asymptotic analysis.

The coupled regime derived in this work may be relevant in problems where a thin interface carries mechanical loads and, at the same time, exchanges chemical species with the surrounding materials. Possible examples include electrolyte–electrode interfaces in battery materials, tissue–implant interfaces involving molecular diffusion, chemically active coatings, and crack or corrosion fronts where stress-assisted diffusion plays a role [22,24,25].

The proposed approach has several limitations. First, it is based on linear chemomechanics and is therefore restricted to small displacement gradients and small deviations of the concentration from its reference value. Second, only the diffusion of a single chemical species is considered. Third, chemical reactions are not included. Fourth, the analysis is restricted to planar interphases. Curved layers would require the introduction of the local frame and the analysis of curvature effects, as done for the elastic case in [38]. Finally, the one-dimensional numerical example is intended to illustrate the qualitative implications of the interface laws, and not to reproduce a specific material system. Moreover, the present analysis is restricted to describe the limit response as the interphase thickness tends to zero. For thin but finite interphases, higher-order corrections may be needed to improve the approximation. However, their derivation would require a dedicated asymptotic analysis and is beyond the scope of the present study.

The proposed methodology can be extended in several directions. A first natural extension concerns thermo-chemoelasticity, where temperature variations would introduce additional couplings among deformation, heat transfer, and species diffusion. A second direction is the treatment of nonlinear material behavior, including finite strains, nonlinear diffusion, chemical reactions, or degradation processes. The analysis could also be extended to more general three-dimensional geometries, including curved interphases, where curvature terms and local surface frames have to be introduced, and to more complex interphase geometries, such as multilayered interphases. In the latter case, each thin layer may have its own stiffness, mobility, storage, and coupling scalings, leading to a richer set of effective interface laws.

Declaration of competing interest

The authors declare the following financial interests/personal relationships which may be considered as potential competing interests: Raffaella Rizzoni is currently serving as Guest Editor of the Special Issue entitled “Multiscale asymptotic methods in solid mechanics”. Given her role as Guest Editor, she had no involvement in the peer review of this article and had no access to information regarding its peer review. Full responsibility for the editorial process for this article was delegated to another journal editor. She declares that she has no known competing financial interests or personal relationships that could have appeared to influence the work reported in this paper.

Acknowledgments

RR gratefully acknowledges the support of the project LESSGAS (CUP: B79J25000600005 - COR: 24519183). This research was done according to the scientific principles of the Italian National Group for the Mathematical Physics (GNFM) of the National Institute for Advanced Mathematics (INdAM). The author is grateful to Andrea Balbo for helpful conversations on surface excess and stress corrosion.

Data availability

No data was used for the research described in the article.

References

[1] A. Maurel-Pantel, M. Lamberti, M.L. Raffa, C. Suarez, F. Ascione, F. Lebon, Modelling of a GFRP adhesive connection by an imperfect soft interface model with initial damage, Compos. Struct. 239 (2020) 112034, http://dx.doi.org/10.1016/j.compstruct.2020.112034.

[2] M. Lamberti, A. Maurel-Pantel, F. Lebon, F. Ascione, Cyclic behaviour modelling of GFRP adhesive connections by an imperfect soft interface model with damage evolution, Compos. Struct. 279 (2022) 114741, http://dx.doi.org/10.1016/j.compstruct.2021.114741.

[3] M.L. Raffa, V.-H. Nguyen, G. Haiat, Micromechanical modeling of the contact stiffness of an osseointegrated bone–implant interface, Biomed. Eng. Online 18 (2019) 114, http://dx.doi.org/10.1186/s12938-019-0733-3.

[4] Z. Hashin, Thermoelastic properties of fiber composites with imperfect interface, Mech. Mater. 8 (1990) 333–348, http://dx.doi.org/10.1016/0167-6636(90)90051-G.

[5] Z. Hashin, Thermoelastic properties of particulate composites with imperfect interface, J. Mech. Phys. Solids 39 (1991) 745–762, http://dx.doi.org/10.1016/0022-5096(91)90023-H.

[6] Y. Benveniste, T. Miloh, Imperfect soft and stiff interfaces in two-dimensional elasticity, Mech. Mater. 33 (2001) 309–323, http://dx.doi.org/10.1016/S0167-6636(01)00055-2.

[7] A. Klarbring, Derivation of a model of adhesively bonded joints by the asymptotic expansion method, Internat. J. Engrg. Sci. 29 (1991) 493–512, http://dx.doi.org/10.1016/0020-7225(91)90053-F.

[8] G. Geymonat, F. Krasucki, S. Lenci, Mathematical analysis of a bonded joint with a soft thin adhesive, Math. Mech. Solids 4 (1999) 201–225, http://dx.doi.org/10.1177/108128659900400204.

[9] F. Lebon, R. Rizzoni, Asymptotic analysis of a thin interface: The case involving similar rigidity, Internat. J. Engrg. Sci. 48 (2010) 473–486, http://dx.doi.org/10.1016/j.ijengsci.2009.12.001.

[10] F. Lebon, R. Rizzoni, Asymptotic behavior of a hard thin linear elastic interphase: An energy approach, Int. J. Solids Struct. 48 (2011) 441–449, http://dx.doi.org/10.1016/j.ijsolstr.2010.10.006.

[11] R. Rizzoni, S. Dumont, F. Lebon, E. Sacco, Higher order model for soft and hard elastic interfaces, Int. J. Solids Struct. 51 (2014) 4137–4148, http://dx.doi.org/10.1016/j.ijsolstr.2014.08.005.

[12] O.L. Cruz-González, R. Rodríguez-Ramos, F. Lebon, F.J. Sabina, Modeling of imperfect viscoelastic interfaces in composite materials, Coatings 12 (2022) 705, http://dx.doi.org/10.3390/coatings12050705.

[13] C. Bauzet, S. Dumont, F. Lebon, F. Nabet, Toward stochastic imperfect interfaces, Z. Angew. Math. Mech. 105 (2025) e70030, http://dx.doi.org/10.1002/zamm.70030.

[14] M.L. Raffa, F. Lebon, G. Vairo, Normal and tangential stiffnesses of rough surfaces in contact via an imperfect interface model, Int. J. Solids Struct. 87 (2016) 245–253, http://dx.doi.org/10.1016/j.ijsolstr.2016.01.025.

[15] M. Serpilli, Classical and higher order interface conditions in poroelasticity, Ann. Solid Struct. Mech. 11 (2019) 1–10, http://dx.doi.org/10.1007/s12356-019-00052-5.
[16] M. Serpilli, R. Rizzoni, F. Lebon, S. Dumont, An asymptotic derivation of a general imperfect interface law for linear multiphysics composites, Int. J. Solids Struct. (2019) 180–181, http://dx.doi.org/10.1016/j.ijsolstr.2019.07.014.
[17] M. Serpilli, S. Dumont, R. Rizzoni, F. Lebon, Interface models in coupled thermoelasticity, Technologies 9 (2021) 17, http://dx.doi.org/10.3390/technologies9010017.
[18] G. Mishuris, Y. Protserov, N. Vaysfeld, Z. Zhuravlova, On atypical imperfect transmission conditions for thin poroelastic interphase, J. Math. Sci. 298 (2026) 208–224, http://dx.doi.org/10.1007/s10958-025-08066-8.
[19] L. Anand, 2014 drucker medal paper: A derivation of the theory of linear poroelasticity from chemoelasticity, J. Appl. Mech. 82 (2015) 111005, http://dx.doi.org/10.1115/1.4031049.
[20] S.A. Chester, C.V. Di Leo, L. Anand, A finite element implementation of a coupled diffusion-deformation theory for elastomeric gels, Int. J. Solids Struct. 52 (2015) 1–18, http://dx.doi.org/10.1016/j.ijsolstr.2014.08.015.
[21] X. Zhang, Z. Zhong, A coupled theory for chemically active and deformable solids with mass diffusion and heat conduction, J. Mech. Phys. Solids 107 (2017) 49–75, http://dx.doi.org/10.1016/j.jmps.2017.06.013.
[22] C.V. Di Leo, E. Rejovitzky, L. Anand, A Cahn–Hilliard-type phase-field theory for species diffusion coupled with large elastic deformations: application to phase-separating li-ion electrode materials, J. Mech. Phys. Solids 70 (2014) 1–29, http://dx.doi.org/10.1016/j.jmps.2014.05.001.
[23] C. Liebl, M. Johlitz, B. Yagimli, A. Lion, Three-dimensional chemo-thermomechanically coupled simulation of curing adhesives including viscoplasticity and chemical shrinkage, Comput. Mech. 49 (2012) 603–615, http://dx.doi.org/10.1007/s00466-011-0663-9.
[24] G.N. Xu, L. Yang, Y.C. Zhou, Z.P. Pi, W. Zhu, A chemo-thermo-mechanically constitutive theory for thermal barrier coatings under CMAS infiltration and corrosion, J. Mech. Phys. Solids 133 (2019) 103710, http://dx.doi.org/10.1016/j.jmps.2019.103710.
[25] F. Zanotto, V. Grassi, A. Balbo, C. Monticelli, F. Zucchi, Stress corrosion cracking of LDX 2101® duplex stainless steel in chloride solutions in the presence of thiosulphate, Corros. Sci. 80 (2014) 205–212, http://dx.doi.org/10.1016/j.corsci.2013.11.028.
[26] A.W. Adamson, A.P. Gast, Physical Chemistry of Surfaces, sixth ed., Wiley-Interscience, New York, 1997.
[27] L. Zhou, W. Liu, Z. Fan, Y. Mao, S. Hou, Chemo-mechanical behaviors of particle enforced heterogeneous composites with chemical interfacial jumps, Int. J. Solids Struct. 239–240 (2022) 111439, http://dx.doi.org/10.1016/j.ijsolstr.2022.111439.
[28] K.L. Auth, J. Brouzoulis, M. Ekh, A fully coupled chemo-mechanical cohesive zone model for oxygen embrittlement of nickel-based superalloys, J. Mech. Phys. Solids 164 (2022) 104880, http://dx.doi.org/10.1016/j.jmps.2022.104880.
[29] S. D'Andréa, S. Lejeunes, F. Lebon, V. Blanc, M. Lainet, A traction-separation interface model for chemical bonding and damage in a thermo-mechanical context, Comput. Mech. (2026) http://dx.doi.org/10.1007/s00466-026-02759-w.
[30] M.E. Gurtin, E. Fried, L. Anand, The Mechanics and Thermodynamics of Continua, Cambridge University Press, Cambridge, 2010.
[31] M.K. Brun, E. Ahmed, J.M. Nordbotten, F.A. Radu, Well-posedness of the fully coupled quasi-static thermo-poroelastic equations with nonlinear convective transport, J. Math. Anal. Appl. 471 (2019) 239–266, http://dx.doi.org/10.1016/j.jmaa.2018.10.074.
[32] R.E. Showalter, Diffusion in poro-elastic media, J. Math. Anal. Appl. 251 (2000) 310–340, http://dx.doi.org/10.1006/jmaa.2000.7048.
[33] P.G. Ciarlet, Mathematical Elasticity. Volume II: Theory of Plates, in: Studies in Mathematics and its Applications, Vol. 27, Elsevier, Amsterdam, 1997.
[34] P.L. Kapitza, Heat transfer and superfluidity of helium II, Phys. Rev. 60 (1941) 354–355, http://dx.doi.org/10.1103/PhysRev.60.354.
[35] A. Ch, Mitropoulos and what is a surface excess? J. Eng. Sci. Technol. Rev. 1 (2008) 1–3, http://dx.doi.org/10.25103/jestr.011.01.
[36] W.E. Schiesser, G.W. Griffiths, A Compendium of Partial Differential Equation Models: Method of Lines Analysis with Matlab, Cambridge University Press, Cambridge, 2009, http://dx.doi.org/10.1017/CBO9780511576270.
[37] The MathWorks Inc., MATLAB version 24.1.0.2578822 (R2024a) [software], Natick, MA, 2024.
[38] R. Rizzoni, F. Lebon, Imperfect interfaces as asymptotic models of thin curved elastic adhesive interphases, Mech. Res. Commun. 51 (2013) 39–50, http://dx.doi.org/10.1016/j.mechrescom.2013.04.008.